Interuniversity Institute for Biostatistics
and statistical Bioinformatics

I-BioStat, here represented by:
Center for Statistics
Hasselt University
Agoralaan 1, Building D
B-3590 Diepenbeek, Belgium
(https://ibiostat.be)
(https://www.uhasselt.be/en/instituten-en/dsi)

FINAL STUDY REPORT

Title: **Benefit Risk contextualisation of COVID-19 vaccines in the EU**
Reference: ROC23 under FWA EMA/2017/09/PE (Lot1)
Deliverable 4 v2_20042022

To:
European Medicines Agency (EMA)
Amsterdam, The Netherlands

PASS information

Title	**Benefit Risk contextualisation of COVID-19 vaccines in the EU**
Version identifier of the final study report	Not applicable
Date of last version of the final study report	Final version expected in February 2022
EU PAS register number	EUPAS44229
Active substance	Tozinameran, Elasomeran, ChAdOx1-S and Ad26.COV2-S
Medicinal product	COVID-19 vaccines by Pfizer (Comirnaty), Moderna (Spikevax), AstraZeneca (Vaxzevria), Johnson & Johnson
Product reference	J07BX (covid-19 vaccines)
Procedure number	Not applicable
Marketing authorisation holder(s)	BioNTech Manufacturing GmbH, Moderna Biotech Spain S.L., AstraZeneca AB and Janssen-Cilag International NV
Joint PASS	No
Research question and objectives	The main objective is to quantify both the benefits and the risks related to COVID-19 vaccines given potential data limitations and reflecting uncertainty with regard to the various ingredients of the proposed risk-benefit measure.
Country or countries of study	Europe
Author	Steven Abrams, Jonas Crèvecoeur, Niel Hens, Neilshan Loedy, Geert Molenberghs, Johan Verbeeck, Lander Willem

Contents

1 Abstract

Introduction The main public health priority during the pandemic is maintaining mortality as low as possible and minimising pandemic induced health and economic distress. To achieve this goal, several vaccines against SARS-CoV-2 induced COVID-19 disease were developed rapidly, all while adhering to stringent quality standards. COVID-19 vaccines are highly effective in lowering the risk of contracting and spreading the virus, as well as lowering the severity of symptoms, thereby decreasing the overall COVID-19 disease burden.

Objectives To propose a method to quantify the benefits and risks of COVID-19 vaccines and to develop a user tool for assessing this benefit-risk, using myocarditis, pericarditis and thrombosis with thrombocytopenia (TTS) as adverse events of interest.

Methods Using a probabilistic model to account for differential vaccine effectiveness and temporal differences in disease dynamics, the benefit of different vaccines in the European Economic Area (EEA) were calculated by comparing the observed number of confirmed cases, hospitalisations, ICU admissions and deaths (source ECDC) with the expected number of these events, had no COVID-19 vaccines been available. Risks of myocarditis, pericarditis and TTS associated with the vaccines was evaluated by comparing the observed risk events (source EudraVigilance) to the expected events based on background incidence rates (source EMA).

Results The vaccines under study had comparable benefits, but magnitude differed by age group, gender and vaccine product. When relying on published vaccine effectiveness estimates, the benefit of vaccination was estimated by the prevention of 13,322,567 confirmed COVID-19 infections, 933,230 COVID-19 hospitalisations, 150,106 ICU admissions and 220,880 COVID-19 related deaths in the EEA, since the start of vaccination. While there was an increased risk of myocarditis in the male population < 40 years of age after Spikevax vaccination, the vaccine prevented substantial COVID-19 hospitalisations in this population. Both the number of clinical benefits, as well as the risk of TTS after Vaxzevria vaccination were the highest in the 60 to 69 years of age category, with benefits outweighing the risk.

Conclusions This analysis demonstrates that the benefits of COVID-19 vaccination far outweigh the myocarditis, pericarditis and TTS risks. Rare, life-threatening side effects associated with vaccination might not be observed in a clinical trial and should be investigated as soon as possible after introduction of vaccines into large populations. The proposed methodology can be applied to any serious adverse event that may occur in the future or other vaccines.

2 List of Abbreviations

Abbreviation	Meaning
ADVANCE	Accelerated development of vaccine benefit-risk collaboration in Europe
AMM	Adaptive Mixture Metropolis-Hastings
AMWG	Adaptive Metropolis within Gibbs
ARS	Agenzia Regionale di Sanità della Toscana
BIFAP	Base de Datos para la Investigación Farmacoepidemiológica en Atención Primaria
COVID-19	Coronavirus Disease 2019
ECDC	European Centre for Disease Prevention and Control
EEA	European Economic Area
EMA	European Medicines Agency
EU	European Union
EudraVigilance	European Union Drug Regulating Authorities Pharmacovigilance
GAM	Generalized Additive Model
GISAID	Global Initiative on Sharing Avian Influenza Data
GPC	Generalized Pairwise Comparison
ICU	Intensive Care Unit
IMI	Innovative medicine initiative
IR	Incidence Rate
ISPOR	International Society for Pharmacoeconomics and Outcomes Research
MCDA	Multi Criteria Decision Analysis
MCMC	Markov Chain Monte Carlo
mRNA	Messenger Ribonucleic Acid
NPIs	Non-pharmaceutical Interventions
ODEs	Ordinary Differential Equations
PCR	Polymerase Chain Reaction
PM	Probabilistic Model
PROTECT	Pharmacoepidemiological Research on Outcomes of Therapeutics
QALY	Quality-Adjusted Life-Year
RWM	Random-Walk Metropolis
SARS-CoV-2	Severe Acute Respiratory Syndrome Coronavirus-2
SCM	Stochastic Compartmental Model
SEIR	Susceptible-Exposed-Infectious-Removed
SMAA	Stochastic Multi criteria Acceptability Analysis
TESSy	the European Surveillance System
TTS	Thrombosis with thromboycytopenia
UMBRA	Unified Methodologies for Benefit-Risk Assessment
VoCs	Variants of Concerns
WAIFW	Who-Acquires-Infection-From-Whom

3 Investigators

Principal investigator: Prof. dr. Geert Molenberghs
Co-investigators: Prof. dr. Niel Hens, Prof. dr. Steven Abrams, Prof. dr. Lander Willem, dr. Jonas Crèvecoeur, Neilshan Loedy, Johan Verbeeck

4 Background and Rationale

The ongoing SARS-CoV-2/COVID-19 pandemic, which caused the first patients with severe breathing problems to be hospitalized between December 2019 and January 2020 in Wuhan, China, rapidly became a worldwide health problem after the first reported case of this novel pneumonia. Moreover, it forced countries worldwide to take strong mitigation measures to prevent a collapse of health care systems and to avert excess COVID-19 related deaths. Despite these mitigation measures, the impact of the pandemic worldwide is overwhelming, with over 400 million officially registered SARS-CoV-2 infections and more than 5,7 million officially reported COVID-19 related deaths on December 17th, 2021 [1]. The true death toll of the COVID-19 pandemic is arguably 3–4 times higher due to under-reporting of deaths in certain regions [2].

As the pandemic continued to bring health and economic hardship, keeping mortality as low as possible was the highest priority. Consequently, governments were forced to put in place measures, referred to as non-pharmaceutical interventions (NPIs), to mitigate the epidemic's impact, thereby minimizing the inevitable economic downturn [3]. While NPIs (e.g., social distancing, increased hygiene, face-and-mouth mask mandates, ...) control the pandemic with variable success, in part depending on the degree of adherence to these measures, vaccines against the SARS-CoV-2-virus induced COVID-19 disease were developed at an unprecedented speed, without compromising the required quality, safety and efficacy regulations [4]. This has led to several approved and licensed COVID-19 vaccines to date.

The European Medicines Agency (EMA) and the European Centre for Disease Prevention and Control (ECDC) jointly coordinate and oversee observational studies on monitoring the safety (i.e., by the EMA), and the effectiveness (ECDC) of these licensed vaccines. While interim reports of effectiveness indicated that vaccination against COVID-19 decreases the rate of infection with the original SARS-CoV-2 strain by at least 80%, reduces the viral load four-fold and reduces the risk of transmission [5], the real-life evidence showed initially vastly decreasing PCR-confirmed SARS-CoV-2 infections in many regions and especially in those age groups with a high vaccine uptake and completed (two-dose, except for Johnson&Johnson, where a single dose applies) vaccination schedule [6]. In the meantime, the performance of the COVID-19 vaccines has been influenced by the emergence of new so-called Variants of Concern (VoCs) and vaccine protection has been declining (waning) due to loss of vaccine-induced immunity, which is evidenced in measurements of humoral immunity. However, the aforementioned early results confirm the expectation of long-lasting stable control of the COVID-19 pandemic, relying on booster vaccination campaigns, which could not be achieved with NPIs alone.

However, with the large-scale roll-out of vaccination across the world in the entire adult population, and in some cases large portions of the minor population (or at least within industrialized countries), close post-marketing monitoring thereof is required, similar to any marketed medication, in order to evaluate

side effects, which cannot be observed in a highly selected experimental study population, that is, however large, still limited in size relative to the post-marketing scale of the operation. Although the majority of side effects following vaccination are transitory and non-severe in nature, potential rare life-threatening side effects can occur and should be documented, investigated and alerted timely. Currently, more than 10 billion doses of a COVID-19 vaccine have been administered worldwide [1] and two safety signals have been further investigated by the EMA, concerning thromboembolic events [7, 8] on the one hand and myocarditis and pericarditis [9] on the other hand. These studies are key to generate adequate evidence to support continuous assessment and evaluation of the benefits of vaccines and health risks involved after vaccination. Next to that, these studies need to inform decision-making on the use of different vaccines in national or regional vaccination strategies among different populations.

5 Research Questions and Objectives

The main objective addressed in this report is the **quantification of both the benefits and the risks related to various COVID-19 vaccines** given potential data limitations and reflecting uncertainty with regard to the various ingredients of the proposed risk-benefit measure.

To facilitate these benefit-risk analyses an interactive Shiny R application is developed and available for use by designated stakeholders.

Finally, we critically reflect on existing and potential future benefit-risk composite measures for correlated and overlapping events (see Section 8).

6 Methodology for Benefit and Risk Quantification

Benefits of COVID-19 vaccination are quantified in terms of the averted number of confirmed COVID-19 cases, prevented number of hospitalizations, ICU admissions and deaths relying on country-specific (age- and) time-specific data with respect to these endpoints.

The benefits are offset against the following potential risks:

- Myocarditis & pericarditis for the mRNA vaccines (Comirnaty and Spikevax), 14 days after vaccination.
- Thrombosis with thrombocytopenia (TTS) for the adenovirus vaccine Vaxzevria, 30 days after vaccination.

In the remainder of this section, we provide an outline of the methodology used to infer benefits and risks of COVID-19 vaccination based on available data sources. Although two different approaches are described for the benefits side, i.e., a probabilistic model and a stochastic compartmental modeling approach, the use of the latter is hampered by the lack of detailed country-specific hospital admission data over time and

by age group. Hence, the results and the Shiny application rely only on the probabilistic model. We will come back to the advantages and disadvantages of both approaches in more detail in Section 9.

6.1 Benefit: Probabilistic Model (PM)

Quantification of the benefits associated with COVID-19 vaccination can be done directly by comparing the observed number of confirmed COVID-19 cases, hospitalizations and deaths with the expected number of the aforementioned events in the counterfactual case that no COVID-19 vaccination would have been present. In order to do so, we perform a by-country assessment of the observed events and the probability of being protected through vaccination at that moment in time. More specifically, we consider a probabilistic model (PM) that accounts for differential vaccine effectiveness after vaccination as a function of time since vaccination, emergence of new variants of concern and age-specific and temporal differences in disease dynamics.

We use a so-called "leaky" vaccination approach. For example, vaccination with 50% vaccine effectiveness (against infection), implies that for a vaccinated individual the likelihood to acquire infection is 50% less as compared to a non-vaccinated individual of the same age and at the same calendar time. As such, we do include breakthrough infections after vaccination in our analysis.

6.1.1 Basic implementation

The implementation of the PM is based on the following reasoning. Let $n(a,t)$ denote the number of confirmed COVID-19 cases at time t and age group a. The (counterfactual) number of confirmed cases in the absence of vaccination would then be equal to:

$$n^*(a,t) = \frac{n(a,t)}{1-\phi(a,t-d)},$$

where $\phi(a,t-d)$ represents the proportion of individuals of age protected through vaccination(or age group) a at time $t-d$, and with d a fixed delay between time of SARS-CoV-2 infection and COVID-19 confirmation. In the ensuing analysis, we consider the delay d to be equal to zero. Note that this assumption implies that the counterfactual number of confirmed cases is directly related to the number of reported cases at the same calendar time, without accounting for a delay between infection and reporting. Although this assumption is unrealistic, the impact thereof on the results is negligible (results not shown), given the fact that the build-up of protection as a result of vaccination is sufficiently slow in relation to the maximum delay between infection and confirmation of infection.

The aforementioned expression can be obtained as follows:

$$n(a,t) = [c_{t-d}(a)n^*(a,t)] + \{[1-v_{t-d}(a)]\, n^*(a,t)\},$$

with the first term representing the contribution of breakthrough infections after vaccination up to time $t-d$, a proportion denoted by $c_{t-d}(a)$, and the second term being the contribution of unvaccinated

individuals (until time $t-d$) becoming infected, i.e., $1-v_{t-d}(a)$, and

$$c_t(a) = \sum_{k=0}^{t} p_k(a)(1-\mathsf{ve}_{(t-k)}),$$
$$v_t(a) = \sum_{k=0}^{t} p_k(a),$$

where

- $p_k(a)$ represents the proportion of vaccinated individuals in age group a at time k (with discrete time steps of one day), and
- $\mathsf{ve}_{(t-k)}$ is the vaccine effectiveness as a function of the time since vaccination equal to $t-k$.

Consequently, we have

$$\begin{aligned} n(a,t) &= \{c_{t-d}(a) + [1-v_{t-d}(a)]\}\, n^*(a,t) \\ &= [1-\phi(a,t-d)]n^*(a,t). \end{aligned}$$

The proportion of protected individuals in age group a at time t is computed as follows:

$$\phi(a,t) = v_t(a) - c_t(a) = \sum_{k=0}^{t} p_k(a)\mathsf{ve}_{(t-k)}.$$

The proportion of vaccinated individuals in the age group a at time t is derived from available vaccine uptake data. The vaccine effectiveness function is considered to have the following functional form:

$$\mathsf{ve}_{(t-k)} = \mathsf{ve}^* \left\{1+\exp\left(-k_0^*\left[(t-k)-x_0\right]\right)\right\}^{-1} \exp\left(-\omega\left[(t-k)-2x_0\right]_+\right).$$

This implies a logistic growth after vaccination to reach a level of protection equal to ve^*, after which an exponential decay takes place with waning rate equal to ω. The operator $[\cdot]_+$ equals zero if the argument is negative and takes the value of the argument when positive. The parameter x_0 represents the midpoint of the logistic growth curve.

Based on the difference between $n^*(a,t)$ and $n(a,t)$ one can estimate the prevented number of COVID-19 cases in age group a at time t. More specifically, the number of prevented cases can be expressed as $\phi(a,t-d)n^*(a,t)$.

6.1.2 Vaccine types

The European regulatory body has granted emergency use authorization to several vaccines, including those developed by Pfizer-BioNTech, Janssen, Moderna, and Oxford-AstraZeneca. Clinical trials and evaluations of mass vaccination campaigns have shown that two doses given three to four weeks apart, or a single

dose for Janssen, can provide high levels of protection against symptomatic and severe disease [10]. In order to take the protection after second dose vaccination into account, we allowed for differential vaccine effectiveness estimates for the mRNA and adeno-based vaccines. Note that in the toolkit, a vaccine brand specific analysis is included, without grouping these vaccine brands into mRNA and adeno-based vaccines, but for the demonstration of the methodology we keep the aforementioned terminology in place.

Consequently, we have

$$\begin{aligned}\phi(a,t) &= \phi^{(1)}(a,t) + \phi^{(2)}(a,t) \\ &= \sum_{k=0}^{t} \left\{ p_k^{(1)}(a)\mathsf{ve}_{(t-k)}^{(1)} + p_k^{(2)}(a)\mathsf{ve}_{(t-k)}^{(2)} \right\}, \end{aligned} \tag{1}$$

with superscripts referring to (1) mRNA- or (2) adeno-based vaccination.

Next to an overall assessment of the impact of vaccination on confirmed cases, hospitalizations, ICU admissions and deaths, a vaccine-type specific approach could be considered as well. Based on the terminology introduced above, we established the relation

$$n(a,t) = \left[1 - \phi(a, t-d)\right] n^*(a,t),$$

where $\phi(a,t-d) = \phi^{(1)}(a,t-d) + \phi^{(2)}(a,t-d)$. Assume that we want to study the impact of vaccination with mRNA vaccines on the number of confirmed COVID-19 cases. In that case, the counterfactual number of confirmed cases, in the absence of mRNA vaccination, is equal to

$$n^{(2)*}(a,t) = \left[1 - \phi^{(2)}(a,t-d)\right] n^*(a,t),$$

and the prevented number of confirmed cases by mRNA vaccines only equals

$$n^*(a,t) - n^{(2)*}(a,t) = \phi^{(2)}(a,t-d) n^*(a,t).$$

Similarly, the prevented number of confirmed cases by adeno-based vaccination equals

$$n^*(a,t) - n^{(1)*}(a,t) = \phi^{(1)}(a,t-d) n^*(a,t).$$

As a result, the total number of prevented confirmed COVID-19 cases, i.e., $\phi(a,t-d)n^*(a,t)$ (see Section 6.1.1), is exactly equal to the prevented cases using mRNA and adeno-based vaccines separately, i.e.,

$$\begin{aligned} n^*(a,t) - n^{(1)*}(a,t) + n^*(a,t) - n^{(2)*}(a,t) &= 2n^*(a,t) - \left[n^{(1)*}(a,t) + n^{(2)*}(a,t)\right] \\ &= 2n^*(a,t) - n^*(a,t)\left[2 - \phi(a,t-d)\right] \\ &= n^*(a,t)\left\{2 - \left[2 - \phi(a,t-d)\right]\right\} \\ &= \phi(a,t-d)n^*(a,t) \end{aligned}$$

A similar strategy can be considered for other endpoints such as hospitalizations, ICU admissions and deaths by decomposing protection against these clinical outcomes by vaccine type.

6.1.3 Variants of Concern

Vaccines can help to reduce disease burden in a variety of ways, including preventing infection, making infected people less infectious, and avoiding severe outcomes in those who are infected, all of which reduce the overall number of infected people and the proportion of symptomatic infections [11]. Nonetheless, the emergence of VoCs has resulted in lower vaccine effectiveness, hence, leading to re-emergence of the disease. In the calculation of the prevented confirmed COVID-19 cases, a change in vaccine effectiveness is allowed for in relation to the prevalence of α and δ VoCs in the population under study. The following correction factor was used:

$$\psi(a,t) = \{1 - p_{\alpha,t}(a) - p_{\delta,t}(a)\} + p_{\alpha,t}(a)\frac{\mathsf{ve}^*_\alpha}{\mathsf{ve}^*} + p_{\delta,t}(a)\frac{\mathsf{ve}^*_\delta}{\mathsf{ve}^*}.$$

These prevalences $p_{\alpha,t}(a)$ and $p_{\delta,t}(a)$ are estimated based on available GISAID data [12, 13, 14]. The GISAID EpiCoV dataset includes genomic surveillance data obtained from sequencing COVID-19 positive samples. In order to estimate the prevalences $p_{\alpha,t}(a)$ and $p_{\delta,t}(a)$ we consider a generalized additive model (GAM) for binary outcome data (e.g., α VoC or not) with a logit link function [15].

Hence, using the correction factor, the proportion of protected individuals in age group a at time t is equal to

$$\phi(a,t) \times \psi(a,t),$$

thereby providing a differential baseline vaccine effectiveness as compared to ve^* for different variants of concern.

6.1.4 Partial vaccine-induced protection after first vaccination

After a first dose of COVID-19 vaccination, individuals already gain (partial) protection against infection, hospitalization and death. However, upon initiation of second dose vaccination in the population, the contribution of first and second dose vaccination to the overall protection in the population should be accounted for. The proportion of protected individuals of age a at calendar time t after first and second vaccination are equal to

$$\phi_1(a,t) = \psi_1(a,t)\sum_{k=0}^{t} p_{1,k}(a)\mathsf{ve}_{1,(t-k)},$$
$$\phi_2(a,t) = \psi_2(a,t)\sum_{k=0}^{t} p_{2,k}(a)\mathsf{ve}_{2,(t-k)},$$

respectively. Here, we have for $l = 1, 2$, dose-specific vaccine effectiveness functions $\mathsf{ve}_{l,(t-k)}$ for which

$$\mathsf{ve}_{1,(t-k)} = \mathsf{ve}_{(t-k)}$$
$$\mathsf{ve}_{2,(t-k)} = \frac{\mathsf{ve}^*_2}{\mathsf{ve}^*} \times \mathsf{ve}_{1,(t-k)},$$

implying that the vaccine effectiveness after the second dose is proportional to the effectiveness after the first dose with time since vaccination. Furthermore, the functions $\psi_1(a,t)$ and $\psi_2(a,t)$ allow for a different correction factor for each of the doses regarding protection against variants of concern.

Note that an extension to include mRNA and adeno-based vaccination is immediate (see above). For ease of presentation, we confine attention to the one vaccine type formulation first. A more detailed description of the expressions in case of multiple vaccine types is presented below.

In order to weigh the contribution of each of the aforementioned expressions in the overall protection in age group a at calendar time t we rely on the proportion of individuals of age a being vaccinated only once or twice in the population, hence, implying that

$$\phi(a,t) = w_{1,t}(a)\phi_1(a,t) + \phi_2(a,t),$$

where $w_{1,t}(a)$ represents the proportion of vaccinated individuals in age group a at time t with a first dose only. More specifically, we have

$$w_{1,t}(a) = \frac{\sum_{k=0}^{t} p_{1,k}(a) - \sum_{k=0}^{t} p_{2,k}(a)}{\sum_{k=0}^{t} p_{1,k}(a)} = \frac{v_{1,t}(a) - v_{2,t}(a)}{v_{1,t}(a)},$$

in terms of the proportion of vaccinated individuals with a first and second dose, respectively. Note that in the absence of protection after the first dose, or when all individuals received their second dose, the formula reduces to $\phi(a,t) = \phi_2(a,t)$. Alternatively, we can write

$$\phi(a,t) = \phi_1(a,t) + \phi_2(a,t)\left\{\frac{v_{1,t}(a) - v_{2,t}(a)\dfrac{\phi_1(a,t)}{\phi_2(a,t)}}{v_{1,t}(a)}\right\},$$

implying an initial increase in protection induced by an increase in protection after second dose vaccination countered by a gradual decrease in protection after first (and second) dose vaccination with time since vaccination. Needless to say, the alternative expression implies that $\phi_2(a,t) \neq 0$. In the absence of second dose vaccination, i.e., $\phi_2(a,t) = 0$, the formula reduces to $\phi(a,t) = \phi_1(a,t)$ as required.

The above formula can be interpreted as follows: the total protection induced by vaccination is the sum of the dose-specific contributions, weighted according the proportion of individuals with a given vaccination uptake (either one dose or two doses).

Considering two vaccine types, i.e., mRNA and adeno-based vaccines, the aforementioned probabilities should be considered vaccine type-specific, leading to

$$\phi(a,t) = \phi^{(1)}(a,t) + \phi^{(2)}(a,t),$$

with, for $j = 1,2$ and $l = 1,2$ denoting mRNA and adeno-based vaccines, and first and second dose, respectively,

$$\phi^{(j)}(a,t) = w_{1,t}^{(j)}(a)\phi_1^{(j)}(a,t) + \phi_2^{(j)}(a,t),$$
$$\phi_l^{(j)}(a,t) = \psi_l^{(j)}(a,t)\sum_{k=0}^{t} p_{l,k}^{(j)}(a)\mathsf{ve}_{l,(t-k)}^{(j)}.$$

Note that this is a generalization of expression (1) in which vaccine types are assumed not be mixed. The functions $\psi_l^{(j)}(a,t)$ are allowed to differ by vaccine dose and vaccine type:

$$\psi_l^{(j)}(a,t) = \{1 - p_{\alpha,t}(a) - p_{\delta,t}(a)\} + p_{\alpha,t}(a)\frac{\mathsf{ve}_{l,\alpha}^{*(j)}}{\mathsf{ve}^{*(j)}} + p_{\delta,t}(a)\frac{\mathsf{ve}_{l,\delta}^{*(j)}}{\mathsf{ve}^{*(j)}}.$$

6.1.5 Additional booster vaccinations

In the presence of additional booster vaccinations, we can rely on a similar approach as considered in Section 6.1.4. More specifically, booster vaccination (using mRNA-based vaccines), denoted hereunder by $b_1, \ldots, b_B$, implies an increase in immunity according to functions $\phi_{b_1}(a,t), \ldots, \phi_{b_B}(a,t)$, with

$$\phi_{b_j}(a,t) = \psi_{b_j}(a,t)\sum_{k=0}^{t} p_{b_j,k}(a)\mathsf{ve}_{b_j,(t-k)}. \tag{2}$$

Note that vaccine properties captured by $\mathsf{ve}_{b_j,(t-k)}$ can be defined differently for booster vaccination $j = 1, \ldots, B$ and that protection is adapted for VoCs depending on their prevalence using $\psi_{b_j}(a,t)$. Note that booster vaccination is presumed to be only of the mRNA type, hence, there is no need to differentiate between booster vaccine types. Consequently, the total immunity in age group a at calendar time t, after first dose booster vaccination, is given by:

$$\phi(a,t) = w_{1,t}^{(1)}(a)\phi_1^{(1)}(a,t) + w_{2,t}^{(1)}(a)\phi_2^{(1)}(a,t) + w_{1,t}^{(2)}(a)\phi_1^{(2)}(a,t) + w_{2,t}^{(2)}(a)\phi_2^{(2)}(a,t) + \phi_{b_1}(a,t),$$

where the weights $w_{1,t}^{(j)}(a)$ and $w_{2,t}^{(j)}(a)$ define the probabilities of having received only a first dose of vaccine type j, or two doses of vaccine type j among vaccinated individuals in age group a at time t. A generalization towards more doses is straightforward by computing the appropriate probabilities.

Calculating the age- and vaccine-type specific burden in the presence of first, second and booster dose vaccination is straightforward and similar to the approach described in Section 6.1.2. For example, the number of prevented cases (first and second dose) as a result of adeno-based or mRNA vaccination is given by $\left\{w_{1,t}^{(2)}(a)\phi_1^{(2)}(a,t) + w_{2,t}^{(2)}(a)\phi_2^{(2)}(a,t)\right\} n^*(a,t)$ or $\left\{w_{1,t}^{(1)}(a)\phi_1^{(1)}(a,t) + w_{2,t}^{(1)}(a)\phi_2^{(1)}(a,t)\right\} n^*(a,t)$, respectively. Consequently, the additional effect of the booster vaccination equals

$$\{\phi_{b_1}(a,t)\}\, n^*(a,t).$$

Essentially, this implies that the prevented burden as a result of first and second dose mRNA and adeno-based vaccination, and the additional prevented burden due to booster vaccination are relative shares of the total prevented burden.

6.1.6 Prevented hospitalizations, ICU admissions and deaths

In the description of the PM methodology, we mainly focused on COVID-19 confirmed cases. However, next to averted cases, we are also interested in prevented hospitalizations, ICU admissions and COVID-19 related deaths as a result of COVID-19 vaccination efforts. Although different approaches are possible to

calculate, for example, the prevented number of hospitalizations (e.g., including an approach translating directly the prevented number of confirmed cases into prevented hospitalizations), we will focus here on an approach directly accounting for the reported number of hospitalizations (ICU admissions or deaths). More specifically, we use an approach which is similar to the approach considered to compute the counterfactual number of confirmed COVID-19 cases.

Using input parameters for vaccine effectiveness against hospitalization, we compute $\phi^H(a,t)$, the proportion of individuals in age group a that are protected against hospitalization at calendar time t. The counterfactual number of hospitalizations is again computed as

$$n^{H*}(a,t) = \frac{n^H(a,t)}{1-\phi^H(a,t-d^H)}.$$

The delay parameter d^H, denoting the delay between hospital admission and infection, is for simplicity set to 0.

The proportion of individuals protected against hospitalization can be expressed as:

$$\phi^H(a,t) = \sum_{k=0}^{t} p_k(a)\mathsf{ve}^H_{(t-k)},$$

where $\mathsf{ve}^H_{(t-k)}$ is the vaccine effectiveness against hospitalization for time since vaccination equal to $t-k$. Vaccine effectiveness against hospitalization is considered to evolve according to a function $\mathsf{ve}^H_{(t-k)}$ which can be considered different from the evolution of vaccine effectiveness against infection with time since vaccination. In the current implementation, a time- and age-invariant re-scaling according to a factor η (i.e., $\mathsf{ve}^H_{(t-k)} = \eta\mathsf{ve}_{(t-k)}$) is considered:

$$\eta = \frac{\mathsf{ve}^{H*}}{\mathsf{ve}^*},$$

with ve^{H*} and ve^* denoting the reported maximal vaccine effectiveness against hospitalization and infection, respectively.

Moreover, the impact of VoCs on the vaccine protection against hospitalization is included in a similar way as for confirmed cases, i.e.,

$$\phi^H(a,t) = \psi^H(a,t)\sum_{k=0}^{t} p_k(a)\mathsf{ve}^H_{(t-k)},$$

with

$$\psi^H(a,t) = \{1-p_{\alpha,t}(a)-p_{\delta,t}(a)\} + p_{\alpha,t}(a)\frac{\mathsf{ve}^{H*}_\alpha}{\mathsf{ve}^{H*}} + p_{\delta,t}(a)\frac{\mathsf{ve}^{H*}_\delta}{\mathsf{ve}^{H*}},$$

with correcting factors potentially being dependent on vaccine dose and vaccine type (see Section 6.1.4).

This method is readily generalizable to other clinical endpoints, however, it requires parameters for vaccine effectiveness against hospitalization (ICU admission, death) and relies on the availability of the number of hospitalizations (ICU admissions, deaths) per age group over time.

6.1.7 Imputation in case of missing data

In order to calculate the counterfactual number of confirmed cases, hospitalizations, ICU admissions and deaths, we require detailed information regarding the vaccine uptake as well as age- and time-specific information on on the burden of disease. However, for some countries such age-specific information was not available (Table 1). To enable the use of the PM for each country and age group, we opted to impute age-specific information based on uniform weights and by relying on the data for other countries for which the required data is available.

Imputing vaccine uptake by age

The default age groups for most countries in the ECDC vaccine tracker were $<$18y, 18-24y, 25-49y, 50-59y, 60-69y, 70-79y and $\geq$80y. To align this with the eight age groups in the PM, we split the reported vaccine uptake uniformly over the included ages. For example the model-based age group 20-30y received $\frac{5}{25}$ of uptake reported for 25-49y. Germany, Liechtenstein and The Netherlands reported their uptake with other age groups. Germany reported the aggregated uptake for all ages below 60 years of age and for all ages equal or above 60 years. As such, we scaled the reported date to the model-based age groups. For example, the age group 60-69y receives $\frac{10}{30}$ of the reported uptake equal or above 60 years of age. For The Netherlands and Liechtenstein, the uptake of all individuals above 18 years of age was aggregated. As such, we scaled the data towards the age groups of the model in line with the description above.

Imputing age-distribution for Liechtenstein

Age-specific population data was not available for Lichtenstein. Therefore, we adopted the age-distribution from the neighboring country Switzerland and weighting the age groups by the total population size of Liechtenstein.

Imputing vaccine brands

For nine countries (Austria, Croatia, Denmark, Finland, France, Germany, Iceland, Lithuania and The Netherlands), there was no vaccine brand data available. As such, we calculated the time- and age-specific proportion of COVID-19 vaccines per brand based on all available vaccine uptake data. Next, we multiplied the reported uptake for the countries with missing data with the overall time- and age-specific proportion of each vaccine brand.

Imputing the total number of hospital and ICU admissions over time

Several countries did not report the daily hospital and ICU admissions, though the confirmed cases over time could be used to fill this gap by using a temporal case-to-hospital and case-to-ICU admission ratio. Based on all available data, we calculated the daily hospital and ICU admission ratio for each country that reported admissions, and used the median value over all countries per day to summarize the process. To smoothen the time-dependent ratios, we continued with a 7-day rolling median value before we imputed missing hospital and ICU admission data based on country-specific reported cases over time. This approach acknowledges that the fraction of confirmed cases that warrants hospital and ICU admissions changed over time due to vaccination, VOC, and other causes. This approach does not account for the delay between infection and hospital admission when looking at the daily numbers. If the final the time resolution is on

weeks, months or years, this limitation is less relevant.

Imputing age-specific burden of disease over time

The available age-specific data on the burden of disease (cases, hospital and ICU admissions, mortality) was limited in time. To enable projections outside this time window, we based the PM on a time-invariant age distribution of hospitalizations, ICU admissions and deaths per country. As such, the temporal age-specific data is aggregated into one age distribution per country. These country-specific age distributions are then multiplied with the total burden of disease over time to obtain age- and time-specific cases, hospitalization, ICU admission and death counts. If there was no country-specific data by age, we relied on the overall age distribution across all countries. See Table 1 for more details on the data availability per country.

Re-scaling of benefit results

Benefits estimated from the PM are scaled to the age categories used for the risk calculations (i.e., as part of the risk input data). Consequently, we presume that the number of vaccinations and benefits by age are equal within each age group. For age groups that are shared for the risk and benefit analysis, this has no consequence. However, for the age category $0-19$, there exists a high risk of bias induced by the fact that vaccination and implied benefits are probably not uniformly distributed across ages in that age group.

6.1.8 Model parameters in the probabilistic model

In this section, we present the default vaccine effectiveness parameters with regard to clinical outcome (i.e., infection, hospitalization, ICU admission and mortality) used throughout the analysis. In Table 2, these vaccine properties are listed by vaccine brand, endpoint and variant of concern. For endpoints for which detailed information was lacking, we consider parameter values from a less severe endpoint respecting the order infection, hospitalization, ICU admission and finally death. As vaccination appears to protect against serious disease caused by all of the major virus types, most vaccinations are less effective against symptomatic sickness due to the delta VoC as compared to the Alpha and Wuhan variants. However, a significant vaccine effectiveness against both symptomatic and severe disease are still observed for the Delta variant. Evidence from recent studies and studies on other corona-viruses suggest that vaccine-induced and natural immunity against SARS-CoV-2 may be short-lived, lasting 6 or 12–18 months, respectively, and depending on a variety of conditions [16]. Needless to say, these parameter values can be altered in the toolkit (based on novel insights described in the scientific literature) to explore the impact thereof on the final benefit-risk quantification.

Country	**Vaccine uptake: age**	**Vaccine uptake: brand**	**Cases**	**Hospital admissions**	**ICU admissions**	**Mortality**
Austria	default	-	time	-	-	time
Belgium	default	reported	time	time, age	-	time, age
Bulgaria	default	reported	time	-	-	time
Croatia	default	-	time	time, age	age	time, age
Cyprus	default	reported	time	time, age	time, age	time, age
Czechia	default	reported	time, age	time, age	time, age	time, age
Denmark	default	-	time, age	time, age	age	time, age
Estonia	default	reported	time	time	time	time
Finland	default	-	time	-	-	time
France	default	-	time	time	time	time
Germany	<60y and ≥60y	-	time, age	time, age	time, age	time, age
Greece	default	reported	time	time	time, age	time, age
Hungary	default	reported	time	age	age	time, age
Ireland	default	reported	time	time, age	time, age	time, age
Iceland	default	-	time	time	time	time
Italy	default	reported	time, age	time	time	time
Latvia	default	reported	time	time	time	time
Liechtenstein	<18y and ≥18y	-	time	time	-	time
Lithuania	default	-	time	-	-	time, age
Luxembourg	default	reported	time	time, age	age	time, age
Malta	default	reported	time	time	time	time
Netherlands	<18y and ≥18y	-	time	time, age	time, age	time, age
Norway	default	reported	time	time, age	time, age	time, age
Poland	default	reported	time	-	-	time, age
Portugal	default	reported	time	-	-	time, age
Romania	default	reported	time	-	-	time
Slovakia	default	reported	time	age	age	time
Slovenia	default	reported	time	time	time	time, age
Spain	default	reported	time	time, age	time, age	time, age
Sweden	default	reported	time	-	-	time

Table 1: Country-specific data availability for vaccine uptake and burden of disease over time and by age. The default vaccine uptake age groups are <18y, 18-24y, 25-49y, 50-59y, 60-69y, 70-79y and ≥80y. We denote missing data with "-".

Table 2: Overview of the default parameters used in the analysis and toolkit. These parameter values correspond to the ve^*, ve^*_α and ve^*_δ parameters mentioned above (allowing for differential protection depending on the vaccine dose).

Vaccine type	Vaccine dose	Variant	Clinical outcome	Value	Source
Comirnaty	Dose 1	Wuhan	Infection	0.52	Creech et al. (2021) [17]
		Alpha		0.48	Bernal et al. (2021) [18]
		Delta		0.36	Bernal et al. (2021) [18]
Comirnaty	Dose 1	Wuhan	Hospitalization	0.89	Creech et al. (2021) [17]
		Alpha		0.83	Stowe et al. (2021) [19]
		Delta		0.94	Stowe et al. (2021) [19]
Comirnaty	Dose 1	Wuhan	ICU admission	0.89	–
		Alpha		0.83	–
		Delta		0.94	–
Comirnaty	Dose 1	Wuhan	Death	0.89	–
		Alpha		0.83	–
		Delta		0.94	–
Comirnaty	Dose 2	Wuhan	Infection	0.95	Creech et al. (2021) [17]
		Alpha		0.94	Bernal et al. (2021) [18]
		Delta		0.88	Bernal et al. (2021) [18]
Comirnaty	Dose 2	Wuhan	Hospitalization	0.95	–
		Alpha		0.95	Stowe et al. (2021) [19]
		Delta		0.96	Stowe et al. (2021) [19]
Comirnaty	Dose 2	Wuhan	ICU admission	0.95	–
		Alpha		0.95	–
		Delta		0.96	–
Comirnaty	Dose 2	Wuhan	Death	0.95	–
		Alpha		0.95	–
		Delta		0.96	–
Comirnaty	Dose 3	Wuhan	Infection	0.95	–
		Alpha		0.94	–
		Delta		0.94	Andrews et al. (2022) [20]
Comirnaty	Dose 3	Wuhan	Hospitalization	0.95	–
		Alpha		0.95	–
		Delta		0.98	Andrews et al. (2022) [20]
Comirnaty	Dose 3	Wuhan	ICU admission	0.95	–
		Alpha		0.95	–
		Delta		0.98	–
Comirnaty	Dose 3	Wuhan	Death	0.95	–
		Alpha		0.95	–
		Delta		0.98	Andrews et al. (2022) [20]
Spikevax	Dose 1	Wuhan	Infection	0.92	Creech et al. (2021) [17]
		Alpha		0.90	Bruxvoort et al. (2021) [21]
		Delta		0.77	Bruxvoort et al. (2021) [21]
Spikevax	Dose 1	Wuhan	Hospitalization	0.92	–

Table 2: Overview of the default parameters used in the analysis and toolkit. These parameter values correspond to the ve^*, ve^*_α and ve^*_δ parameters mentioned above (allowing for differential protection depending on the vaccine dose).

Vaccine type	Vaccine dose	Variant	Clinical outcome	Value	Source
		Alpha		0.90	–
		Delta		0.77	–
Spikevax	Dose 1	Wuhan	ICU admission	0.92	–
		Alpha		0.90	–
		Delta		0.77	–
Spikevax	Dose 1	Wuhan	Death	0.92	–
		Alpha		0.90	–
		Delta		0.77	–
Spikevax	Dose 2	Wuhan	Infection	0.94	Creech et al. (2021) [17]
		Alpha		0.98	Bruxvoort et al. (2021) [21]
		Delta		0.87	Bruxvoort et al. (2021) [21]
Spikevax	Dose 2	Wuhan	Hospitalization	0.98	Creech et al. (2021) [17]
		Alpha		0.98	–
		Delta		0.98	Bruxvoort et al. (2021) [21]; Andrews et al. (2021) [22]
Spikevax	Dose 2	Wuhan	ICU admission	0.98	–
		Alpha		0.98	–
		Delta		0.98	–
Spikevax	Dose 2	Wuhan	Death	0.98	–
		Alpha		0.98	–
		Delta		0.98	–
Spikevax	Dose 3	Wuhan	Infection	0.94	–
		Alpha		0.98	–
		Delta		0.95	Andrews et al. (2022) [20]
Spikevax	Dose 3	Wuhan	Hospitalization	0.98	–
		Alpha		0.98	–
		Delta		0.98	–
Spikevax	Dose 3	Wuhan	ICU admission	0.98	–
		Alpha		0.98	–
		Delta		0.98	–
Spikevax	Dose 2	Wuhan	Death	0.98	–
		Alpha		0.98	–
		Delta		0.98	–
Vaxzevria	Dose 1	Wuhan	Infection	0.64	Creech et al. (2021) [17]
		Alpha		0.49	Bernal et al. (2021) [18]
		Delta		0.30	Bernal et al. (2021) [18]
Vaxzevria	Dose 1	Wuhan	Hospitalization	0.95	Creech et al. (2021) [17]
		Alpha		0.76	Stowe et al. (2021) [19]
		Delta		0.71	Stowe et al. (2021) [19]
Vaxzevria	Dose 1	Wuhan	ICU admission	0.95	–

Table 2: Overview of the default parameters used in the analysis and toolkit. These parameter values correspond to the ve^*, ve^*_α and ve^*_δ parameters mentioned above (allowing for differential protection depending on the vaccine dose).

Vaccine type	Vaccine dose	Variant	Clinical outcome	Value	Source
		Alpha		0.76	–
		Delta		0.71	–
Vaxzevria	Dose 1	Wuhan	Death	0.95	–
		Alpha		0.80	Sonabend et al. (2021) [23]
		Delta		0.80	Sonabend et al. (2021) [23]
Vaxzevria	Dose 2	Wuhan	Infection	0.70	Creech et al. (2021) [17]
		Alpha		0.75	Bernal et al. (2021) [18]
		Delta		0.67	Bernal et al. (2021) [18]
Vaxzevria	Dose 2	Wuhan	Hospitalization	0.98	Creech et al. (2021) [17]
		Alpha		0.86	Stowe et al. (2021) [19]
		Delta		0.92	Stowe et al. (2021) [19]
Vaxzevria	Dose 2	Wuhan	ICU admission	0.98	–
		Alpha		0.86	–
		Delta		0.92	–
Vaxzevria	Dose 2	Wuhan	Death	0.98	–
		Alpha		0.95	Sonabend et al. (2021) [23]
		Delta		0.95	Sonabend et al. (2021) [23]

6.2 Benefit: Stochastic Compartmental Model (SCM)

As mentioned previously, an alternative to the probabilistic model described in Section 6.1 is a (stochastic) compartmental modelling approach. Although we describe this method here to stress its usefulness, lack of granular data prevented us to use the outlined method.

Dynamic transmission models are flexible models that incorporate uncertainty about parameter estimates for relevant quantities and allow for multiple benefits (and risks). These models have been recommended by the IMI-ADVANCE working group [24] and were also recently used in the Janssen thromboembolic benefit-risk assessment [25]. Both the societal perspective, via compartmental models, and the individual perspective, via individual-based models, belong to this family of dynamic transmission models. The models are informed by the same information as the initial method, but (parameter) uncertainty is naturally built in through the use of Bayesian (inferential) methodology. Furthermore, when using a stochastic compartmental model, an additional layer of disease transmission variability can be incorporated. Additional compartments can be created to account for indirect vaccination effects and subjects who have received multiple vaccines, but the models' flexibility necessitates a careful balance of parsimony and general applicability with sufficient granularity. To capture disease dynamics and estimate and project past and future incidence rates in the absence or presence of vaccinations, these mathematical models require a minimum of (incidence) data with a minimum of quality. A mathematical compartmental transmission model can be used to directly calculate the effect of vaccination on hospitalizations and deaths. A compartmental model

divides the entire population into different compartments or disease states, allowing the disease process to be represented.

To describe COVID-19 disease dynamics, we propose an adapted version of an SEIR mathematical compartmental model, which includes a susceptible, exposed, pre- and a/symptomatic state, as well as hospital compartments following symptomatic disease. Furthermore, we include various age groups, with age intervals determined by the resolution of incidence data available (preferably ten-year age groups). In order to develop such a compartmental model, we start from a simplification of the extended age-structured SEIR(-type) compartmental model which has been used to describe SARS-CoV-2 transmission in the Belgian population [26]. Figure 1 graphically depicts a schematic representation of the various disease states in the original model.

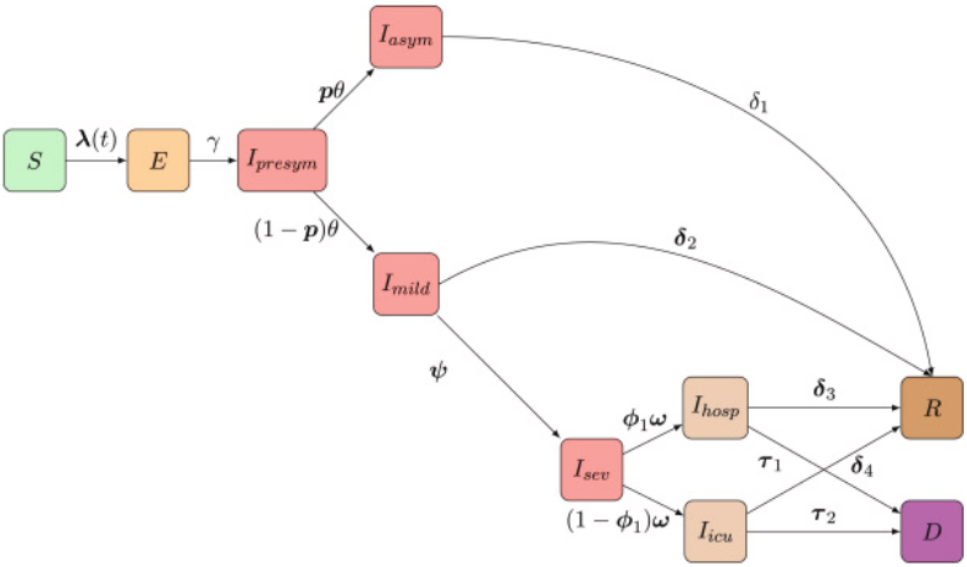

Figure 1: Schematic overview of the flows of individuals in the compartmental model: Following SARS-CoV-2/COVID-19 infection susceptible individuals (S) move to an exposed state (E) and after a latent period individuals further progress to a pre-symptomatic state (I_{presym}) in which they can infect others. Consequently, individuals stay either completely symptom-free (I_{asym}) or develop mild symptoms (I_{mild}). Asymptomatic individuals will recover over time. Upon having mild symptoms, persons either recover (R) or require hospitalization (going from I_{sev} to I_{hosp} or I_{icu}) prior to recovery (R) or death (D)

Abrams et al. [26] calibrated their stochastic discrete-time age-structured compartmental model using high-level hospitalization data, serial serological survey data, and Belgian mortality data. The stochastic model, in more detail, generates (stochastic realizations of) the daily number of new hospitalizations by age group (i.e., 10 year age groups). Individuals are susceptible to infection in this model, and the susceptible individual moves to an exposed state after an effective contact (between a susceptible and infectious individual). The individual becomes infectious and moves to a pre-symptomatic state after a latent period. Individuals either develop symptoms or remain symptom-free following that. Symptomatic infections can

be very mild or very severe, necessitating hospitalization. Patients who are hospitalized or admitted to the Intensive Care Unit (ICU) either recover or die. The following set of ordinary differential equations (ODEs) describes the model transitions:

$$\begin{aligned}
\frac{d\boldsymbol{S}(t)}{dt} &= -\boldsymbol{\lambda}(t)\boldsymbol{S}(t) \\
\frac{d\boldsymbol{E}(t)}{dt} &= \boldsymbol{\lambda}(t)\boldsymbol{S}(t) - \gamma\boldsymbol{E}(t) \\
\frac{d\boldsymbol{I_{presym}}(t)}{dt} &= \gamma\boldsymbol{E}(t) - \theta\boldsymbol{I_{presym}}(t) \\
\frac{d\boldsymbol{I_{asym}}(t)}{dt} &= \theta\boldsymbol{p}\boldsymbol{I_{presym}}(t) - \delta_1\boldsymbol{I_{asym}}(t) \\
\frac{d\boldsymbol{I_{mild}}(t)}{dt} &= \theta(1-\boldsymbol{p})\boldsymbol{I_{presym}}(t) - \{\boldsymbol{\psi} + \boldsymbol{\delta}_2\}\boldsymbol{I_{mild}}(t) \\
\frac{d\boldsymbol{I_{sev}}(t)}{dt} &= \boldsymbol{\psi}\boldsymbol{I_{mild}}(t) - \boldsymbol{\omega}\boldsymbol{I_{sev}}(t) \\
\frac{d\boldsymbol{I_{hosp}}(t)}{dt} &= \boldsymbol{\phi}_1\boldsymbol{\omega}\boldsymbol{I_{sev}}(t) - \{\boldsymbol{\delta}_3 + \boldsymbol{\tau}_1\}\boldsymbol{I_{hosp}}(t) \\
\frac{d\boldsymbol{I_{icu}}(t)}{dt} &= (1-\boldsymbol{\phi}_1)\boldsymbol{\omega}\boldsymbol{I_{sev}}(t) - \{\boldsymbol{\delta}_4 + \boldsymbol{\tau}_2\}\boldsymbol{I_{icu}}(t) \\
\frac{d\boldsymbol{D}(t)}{dt} &= \boldsymbol{\tau_1}\boldsymbol{I_{hosp}}(t) + \boldsymbol{\tau}_2\boldsymbol{I_{icu}}(t) \\
\frac{d\boldsymbol{R}(t)}{dt} &= \delta_1\boldsymbol{I_{asym}}(t) + \boldsymbol{\delta}_2\boldsymbol{I_{mild}}(t) + \boldsymbol{\tau}_3\boldsymbol{I_{hosp}}(t) + \boldsymbol{\delta}_4\boldsymbol{I_{icu}}(t)
\end{aligned}$$

Transmission of the disease is governed by an age- and time-dependent force of infection (k, t), for age group $k = 1, \ldots, K$ at calendar time t, i.e., the instantaneous rate at which a susceptible person in age group k acquires infection at time t. The transmission rate $\beta(k, k', t)$ represents the average per capita rate at which an infectious individual in age group k' makes an effective contact with a susceptible individual in age group k, per unit of time, at calendar time t. Consequently, the force of infection is defined as

$$\lambda(k, t) = \sum_{k'=0}^{K} \beta(k, k', t) I(k', t)$$

where $I(k', t)$ denotes the total number of infectious individuals in age group k' at time t and $\beta(k, k', t)$ can be rendered as $\beta(k, k', t) = q(k, k', t) \times c(k, k', t)$, when relying on the so-called social contact hypothesis [27]. This hypothesis entails that $c(k, k', t)$ are the per capita rates at which an individual in age group k makes contact with an individual in age group k', per unit of time, at calendar time t and q is a proportionality factor capturing contextual and host- and disease-specific characteristics such as susceptibility to infection and infectiousness upon infection. In the absence of detailed social contact data for each of the member states, (age-dependent) transmission rates will be directly estimated by contrasting disease/hospitalization incidence with model-based output given specific values thereof, and potentially relying on a so-called Who-Acquires-Infection-From-Whom (WAIFW) approach to allow for age-heterogeneous transmission (see Hens et al. (2012) [28] for more details thereon).

Model parameters are estimated using a Markov Chain Monte Carlo (MCMC) approach with the model being implemented as a stochastic chain binomial model with transition probabilities being defined in

Abrams et al. [26]. A two-phase method is considered in which the first phase consists of an adaptive Metropolis-within-Gibbs (AMWG) and/or adaptive mixture Metropolis–Hastings (AMM) algorithm to achieve stationary samples that seem to have converged to the target posterior distributions. In the second phase, a non-adaptive Random-Walk Metropolis (RWM) algorithm is used to draw final samples from the posterior distributions.

As an important goal of these compartmental models is the quantification of the impact of vaccination, specific vaccination compartments will be included as an extension of the model depicted in Figure 1, thereby reflecting first and second dose vaccine uptake and potential differential vaccine effectiveness following first and second dose, respectively. The final goal will be to estimate the number of hospitalizations, ICU admission and deaths in the absence of vaccination and to contrast this with observed values, to quantify the prevented clinical events. So far, we did not mention the emergence and circulation of different variants of concern (VoCs) and their potentially increased virulence and disease burden (both in terms of hospitalizations and deaths). Whereas the original compartmental model has been adapted to account for the alpha-variant B.1.1.7 as well as vaccination (see Figure 2); recent adaptations to include the delta-variant B.1.167.2 and the omicron-variant B.1.1.529 warrant the use of more detailed information that will become available during the next weeks and months. As novel VoCs are likely to emerge in the future, a generic way of introducing it into the modeling approach will be considered.

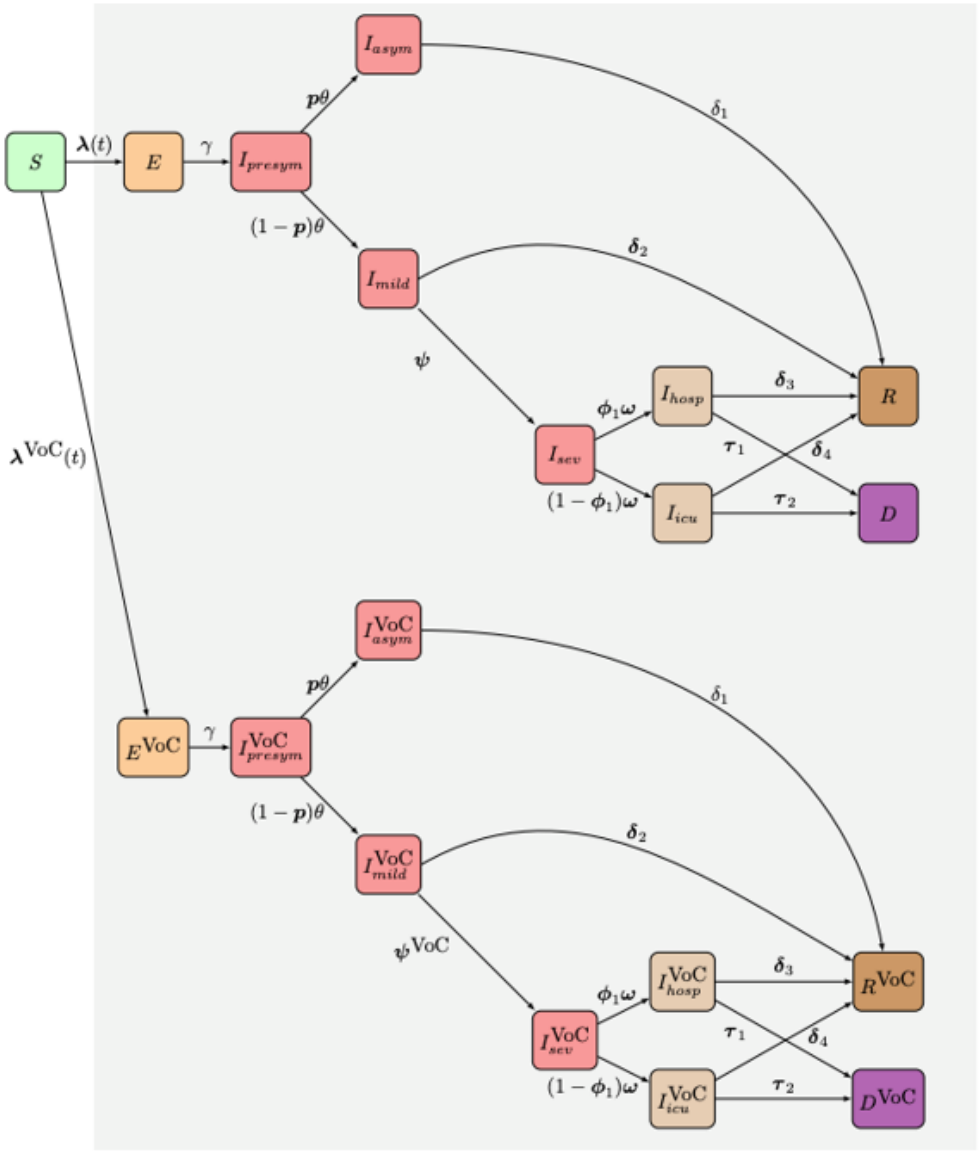

Figure 2: Schematic overview of the flows of individuals in the adapted version of the compartmental model

The emergence of the alpha-variant was accommodated through the inclusion of additional infection states allowing disease features to be different for the alpha-variant as compared to the wild-type. Next to that, the increased transmissibility of the alpha-variant is estimated from Belgian genomic surveillance data. More specifically, the observed prevalence of the alpha-variant is contrasted with model-based predictions under a given transmissibility which is then inferred from the data.

Again, vaccination was accommodated by doubling the different disease states for vaccinated and unvaccinated individuals, in the presence of either the wild-type or VoC. Vaccinated individuals who acquire

infection have a lower risk for COVID-19 related hospital admission. Pending more evidence, we assume an overall reduction of 100% as shown in different vaccine trials [17]. Severe non-hospitalized cases are currently not separately modelled, hence the impact of vaccination on non-hospitalized severe cases, seen in primary care is not separately shown. Vaccine-induced immunity against infection is implemented as a step function with a switch from 0% to 75% protection against infection 21 days after the first dose. Vaccine-induced protection against hospital admission is implemented in the same way using the (higher) estimates reported above. We are able to include differences between mRNA and adenovirus-based vaccines in how they induce immunity and protection. An age-specific uptake scheme can be considered in the model based on available vaccination coverage information from the member states.

Given the complexity of creating a synthetic population for each of the different member states in an individual-based modeling approach, we limit our description to the development and application of a (sufficiently elaborate) compartmental model. In summary, we aim to develop a generic compartmental modeling approach to be applicable to the different member states and to be tailored to the differential availability of data in these countries. A minimum of input data is required to be able to reliably estimate the impact of vaccination in terms of hospital admissions and deaths averted. For more details about the methodology we refer to the description in Abrams et al. [26].

Note that as the compartmental model is used to describe the disease dynamics in the specific population under study, a change in the compartmentalization of the population will not be allowed for. Consequently, the model parameters governing the flows of individuals throughout the system cannot be changed by the member states. The benefit risk-analysis under a set of (plausible) scenarios, where the "epidemiological weather" of a certain point in time/period in time is used, together with key disease-specific factors can be considered. This is in line with our intention to 'borrow' certain conditional information from other countries should it not be available for the country under study. Or, a simpler approach without relying on social contact data could potentially be implemented to circumvent dependence there upon. Given that the most important game changers are VOCs and their characteristics on the one hand and characteristics of the vaccines on the other.

Although the SCM provides a more realistic description of the transmission dynamics, the use of the SCM is hampered by the lack of granular country-level information with regard to the age- and time-specific incidence of hospitalizations (and deaths). In the absence of such granular data, the calibration of the model, i.e., the estimation of (age-specific) transition probabilities (e.g., the probability of hospitalization given COVID-19 infection), is impossible. An overview of the advantages of the SCM as compared to the PM is presented in the Section 9.

6.3 Risk Methodology

6.3.1 Missing Age and/or Gender Information in Reported EudraVigilance Cases

In a small but relevant proportion of the reported EudraVigilance cases information on age and/or gender is missing. By taking the appropriate age and gender proportions of the completely reported EudraVigilance

cases the missing information is imputed.

6.4 Pooling of the Background Rate Estimates Over All Data Sources

When risk background incidence rate (IR) estimates are available from different data sources, a benefit risk assessment can be performed with each of these estimates or the background rates can be pooled. Both the single source as the pooled background rate analyses are feasible in the toolkit. The toolkit automatically calculates the pooled background rates of any number of provided background incidence rate sources using the methodology detailed in this section.

The IR estimates from distinct data sources are pooled by inverse variance (σ^2) weighting so that estimates from a large data source, which are expected to be more precise, will be allowed to have a larger influence on the weighted mean [29]. Additionally, we allow for a manually chosen weight, x, so that more importance can be assigned, if needed, to a data source that is believed to produce more precise estimates (e.g., a primary care data source versus a primary and secondary care data source). The weights are values limited between 0 and 1. The relative ratio of the weights determine the importance, hence weights 0.1/0.1/0.1, will be equal to 0.3/0.3/0.3 and weights 1/0.1/0.1, will give the first estimate 10 times more importance than the latter two estimates.

The variance for the incidence for each age category, gender and data source i combination:

$$\mathsf{IR}_i = \frac{c_i}{t_i} 100,000$$

is obtained from the symmetric Wald confidence limits for count c_i and person-years t_i. The Wald standard deviation $sd_i(c) = \sqrt{c}_i$, such that

$$\sigma_i^2(\mathsf{IR}) = \frac{c_i}{t_i^2} 100,000^2.$$

While the assumption of symmetry may not be entirely verified, for sufficiently large data sets, this is a viable approximation.

A weighted mean $\overline{\mathsf{IR}}$ of the different estimates per data source i can be obtained by:

$$\overline{\mathsf{IR}} = \frac{\sum_{i=1}^{n} \mathsf{IR}_i w_i}{\sum_{i=1}^{n} w_i},$$

with n the number of data sources and

$$w_i = \frac{x_i}{\sigma_i^2}.$$

If $x_i = 0.1$ for each i then each estimate contributes equally. By setting for instance $x_i = 1$ for one data source, the contribution of this data source to the mean will be more important. Finally, for a single source analysis of data source i, the weight for this data source is set to 1, while all other data sources receive a weight of zero.

The variance of the weighted mean is obtained by:

$$\mathrm{Var}(\overline{\mathrm{IR}}) = \frac{\sum_{i=1}^{n} x_i^2}{\left(\sum_{i=1}^{n} w_i\right)^2}.$$

6.4.1 Redistribution of Vaccination Coverage Data

Vaccination coverage data is available via two sources:

- The weekly updated ECDC vaccine tracker, includes weekly vaccine coverage from 27 European countries and Norway, Iceland and Liechtenstein by vaccine brand, dose and age (Age 0–4; **Age 5–9; Age 10–14; Age 15–17**; Age 18–24; **Age 25–49**; Age 50–59; Age 60–69; Age 70–79; Age 80+). Some countries report the vaccine coverage <18 years as an aggregate, while others report only an aggregate of the coverage ≥18 years. Gender information is absent.
- Solicited request (30 September 2021) to European Member States, includes time vaccine coverage of 19 European countries for Vaxzevria (AstraZeneca), Comirnaty (Pfizer), Spikevax (Moderna) (ECDC countries minus Bulgaria (BG), Cyprus (CY), Denmark (DK), Germany (DE), Hungary (HU), Italy (IT), Liechtenstein (LI), Luxembourg (LU), Malta (MT), Poland (PL), Slovakia (SK)) and 15 countries for Janssen (19 countries minus Finland (FI), France (FR), Norway (NO), Sweden (SE)) by vaccine brand, dose, **gender** and age (**Age 5–11; Age 12–15; Age 16–17**; Age 18–24; **Age 25–29; Age 30–39; Age 40–49**; Age 50–59; Age 60–69; Age 70–79; Age 80+). Greece (GR or EL) uses age categories 12–14y and 15–17y rather than 12–15y and 16–17y.

As the ECDC data source contains the most up to date information on the vaccine coverage per country, but lacks gender information, the coverage per gender is imputed from gender proportions obtained from the Member States data. Additionally, a redistribution over some age categories is required as the age categories in the two data sources do not coincide and may differ from the age categories required for the risk assessment. The coverage per gender and required age category is obtained in a pre-processing step outside the toolkit, via two methodologies:

- **Fixed proportions**: Coverage redistribution per age category of countries that report only aggregates to ECDC by the age proportions of the countries that do report coverage per age categories. Subsequently, coverage redistribution by gender and the required age categories by using the Member States gender and age coverage proportions.
- **Multiple imputation**: Coverage redistribution of the ECDC data via multiple imputation to gender and the required age categories by using the Member States age and gender coverage proportions.

Let $n_{c,a_r,s}$ be the vaccination coverage in country c, required age category a_r and gender s. The vaccination coverage is a three-way table of which for some countries only marginal (or aggregated) counts n_{+c,a_r} are observed or in an overlapping age category.

To redistribute the vaccine coverage in the ECDC vaccine tracker to the gender and required age category, the observed vaccine coverage is multiplied with the age gender proportion $\pi_{a,s}$ taken over all countries:

$$n_{c,a_r,s} = n_{c,a_i,s}\pi_{a_r,s},$$

where a_i can be in the required age category a_r or an aggregated or overlapping age category a_k.

For a given age category a, the vaccine coverage $n_{c,a_r,s}$ follows a multinomial distribution with probability $\pi_{a_r,s}$, which can be estimated from the reported marginal (aggregated) counts:

$$\widehat{\pi}_{a_r,s} = \frac{n_{+a_r,s}}{n_{++a_r}}$$

with variance

$$\mathsf{Var}(\widehat{\pi}_{a_r,s}) = \frac{\widehat{\pi}_{a_r,s}(1-\widehat{\pi}_{a_r,s})}{n_{++a_r}}.$$

In the **fixed proportion** redistribution, it is assumed that the vaccine coverage follows the same multinomial distribution in all countries, where the proportion $\widehat{\pi}_{a_r,s}$ is estimated from the Member States data. For countries, where coverage is reported aggregated over age categories a_k, the proportion is additionally multiplied with $\widehat{\pi}_{a_r} = \frac{n_{+a_r}}{n_{+a_k}}$, the proportion of the multinomial age distribution obtained from the ECDC countries with coverage reported by a_r age categories.

In the **multiple imputation** redistribution, it is assumed that the multinomial age-gender distribution of the vaccine coverage in all countries may or may not be equal to the estimate over the Member State countries with reported age categories. The uncertainty in the age-gender distribution, is allowed by drawing $m = 1, \ldots, M$, times $\pi_{s,a}^{(m)}$ from $N\left(\widehat{\pi_{s,a}}, \frac{\widehat{\pi_{s,a}}(1-\widehat{\pi_{s,a}})}{n_{++a}}\right)$ and by subsequently drawing $n_{c,a}$ copies from Binom $\left(\pi_{s,a}^{(m)}\right)$ for the gender redistribution; or by drawing from a multivariate normal distribution with a diagonal variance-covariance matrix and subsequently a multinomial distribution for gender and age category redistribution. Both result in M estimates $n_{c,a,s}^{(m)}$ of the vaccine type coverage in that country, age group and gender.

For the **myocarditis and pericarditis** risk, a redistribution of the ECDC coverage from age categories 5–17/25–49 into the age categories 5–11/12–17/25–29/30–39/40–49 is required, which coincide with the Member State age categories. These age categories thus require multinomial proportions for redistribution to age and gender, while the other age categories require only binomial proportions for redistribution to gender. For the **TTS** risk, a redistribution from age categories 10–17/18–24/25–49 into the age categories 10–19/20–29/30–39/40–49 is required. The vaccination coverage in the age category 18–24 (a) in both the ECDC and Member States data is split to age categories 18–19 and 20-24 (a_k with $k = 1, 2$) by using

population data from EUROSTAT, assuming equal chance of vaccination per age:

$$n_{c,a_k,s} = \frac{n_{c,a,s} P_{c,a_k,s}}{P_{c,a,s}},$$

with $P_{c,a,s}$ the population in country c, age group a and gender s.

The coverage in the age group 5–11 can be spread over the ages in the category using population data, similar to age category 18–24. At the time of reporting, the assumption of equal chance of vaccination per age in this each group is however unlikely. Therefore, it is assumed that an negligible part of Member States have vaccinated < 10 years at the time of reporting, so the age category 5–11 will be assumed to represent vaccine coverage in age category 10–11. For countries where only aggregated information $\geq$18 years is available from ECDC, we will first estimate the coverage < 18 years using the adult-children proportion of the other countries and subsequently estimate the coverage per age category and gender.

6.4.2 Observed-Expected Ratio

In case the **fixed proportions** are used for the redistribution of the vaccine coverage data, the Observed-Expected risk ratio is obtained by:

$$R_{a,s} = \frac{EV_{a,s} 100,000}{\mathsf{IR}_{a,s} n_{a,s} t} \tag{3}$$

with $EV_{a,s}$ the reported risk cases to EudraVigilance, $n_{a,s} = \sum^{c} n_{c,a,s}$ and t the time horizon in years. The confidence interval of the Observed-Expected ratio is obtained by applying the Wilson and Hilferty [30] approximation for chi-square percentiles [31]:

$$LL = \left(1 - \frac{1}{9EV_{a,s}} - \frac{z_{1-\alpha/2}}{3\sqrt{EV_{a,s}}}\right)^3 \frac{EV_{a,s} 100,000}{\mathsf{IR}_{a,s} n_{a,s} t}$$

$$UL = \left(1 - \frac{1}{9(EV_{a,s}+1)} + \frac{z_{1-\alpha/2}}{3\sqrt{EV_{a,s}+1}}\right)^3 \frac{(EV_{a,s}+1) 100,000}{\mathsf{IR}_{a,s} n_{a,s} t}$$

In case **multiple imputation** is used for the redistribution of the vaccine coverage, we have per multiple imputation m, the coverage $n^{(m)}_{c,a,s}$ per vaccine type, age, gender and country and its variance $\mathsf{Var}(n^{(m)}_{c,a,s}) = n^{(m)}_{c,a,s} \pi^{(m)}_{s,a} \left(1 - \pi^{(m)}_{s,a}\right)$.

For each imputation m, the Observed-Expected ratio $R^{(m)}_{a,s}$ per age and gender is obtained by summing $n^{(m)}_{c,a,s}$ and $\mathsf{Var}(n^{(m)}_{c,a,s})$ over all countries, assuming coverage between countries is independent, and by:

$$R^{(m)}_{a,s} = \frac{EV_{a,s} 100,000}{\mathsf{IR}_{a,s} n^{(m)}_{a,s} t}$$

The variance of $R^{(m)}_{a,s}$ consists of the variability of the imputed $n^{(m)}_{a,s}$, with or without the variability of the

pooled $IR_{a,s}$ which are considered independent:

$$\text{Var}\left(R_{a,s}^{(m)}\right) = \left(\frac{EV_{a,s}100,000}{t}\right)^2 \frac{\text{Var}(\text{IR}_{a,s})\text{Var}\left(n_{a,s}^{(m)}\right) + \text{Var}(\text{IR}_{a,s})\left(E\left(n_{a,s}^{(m)}\right)\right)^2 + \text{Var}\left(n_{a,s}^{(m)}\right)(E(\text{IR}_{a,s}))^2}{\left(E(\text{IR}_{a,s})E\left(n_{a,s}^{(m)}\right)\right)^4}.$$

If it is decided not to pool the background risk incidence rates from the various data sources, the Var $(IR_{a,s})$ becomes zero in the above formula.

Finally, the $R_{a,s}^{(m)}$ are combined using Rubin's rule to obtain the observed-risk ratio per age category and gender $\overline{R_{a,s}}$, averaged over the multiple imputation estimates:

$$\overline{R_{a,s}} = \frac{\sum_{m=1}^{M} R_{a,s}^{(m)}}{M},$$

with variability:

$$\text{Var}(R_{a,s}) = \frac{\sum_{m=1}^{M}\text{Var}\left(R_{a,s}^{(m)}\right)}{M} + \left(\frac{M+1}{M}\right)\left(\frac{\sum_{m=1}^{M}\left(R_{a,s}^{(m)} - \overline{R_{a,s}}\right)^2}{M-1}\right).$$

6.4.3 Expected prevented or additional risk burden

Vaccination may cause risk events or prevent risk events associated with both vaccination and COVID-19. The expected prevented or additional burden of vaccination is expressed as the difference between the observed and expected risk events per age category and gender:

$$D_{a,s} = EV_{a,s} - \frac{\text{IR}_{a,s}n_{a,s}t}{100,000}.$$

6.5 Data Sources

The following data sources are used in the analysis:

The incidence dataset
This dataset is obtained from both the EMA as well as the ECDC datasets. It contains information from 20 countries reporting case-based data between January until the end of March 2021 by 10-year age categories (<10, 10-19, ...) for the incidence of confirmed COVID-19 cases, and limited information on hospitalizations, ICU admissions, and COVID-19 related deaths. Note that these data are not available for each of the member states.

Vaccination coverage
The vaccination coverage data comes from the European Union/European Economic Area (EU/EEA) countries' Vaccine Tracker submissions to ECDC via the European Surveillance System (TESSy), de dato 10 February 2022. It contains data on the COVID-19 vaccine roll-out, with each row containing the corresponding data for each targeted study vaccine (Pfizer, AstraZeneca, Moderna, and Johnson & Johnson) for a specific week and country. The data is stratified by several age categories with information regarding the number of doses received (first/second dose). Additionally, a data set with the vaccination coverage requested to the Member States by EMA is available, de dato 30 September 2021. This data set is stratified by vaccine, age categories, gender and dose.

We reformatted age groups in the vaccine uptake data to 10 year age groups and imputed age values if aggregated information was available, e.g., vaccine uptake for age groups ≤ 60 years and > 60 years.

Data on vaccine effectiveness
Literature reviews (e.g., by Bernal et al. (2021) [18] and Vasileiou et al. (2021) [32]) can be used to determine the efficacy of various vaccines against symptomatic disease, COVID-19 hospitalization, COVID-19 ICU admission, and COVID-19 death.

Data on Variants of Concern (VoCs)
The dataset contains data on the volume of COVID-19 sequencing, as well as the number and percentage of variants of concern (VoCs) distributed by week and country (30 countries included) that were submitted to the GISAID EpiCoV database and TESSy since the beginning of May 2020. The dataset also included several VoCs (such as Alpha and Delta), the number of variant detections reported, and the variant percentage.

Background incidence risk
The background incidence risk for Myocarditis & pericarditis are provided by EMA dd. 10 November 2021. The data contains the IR and person-years per age and gender in the period before the COVID-19 pandemic and in the period during the COVID-19 pandemic, but before vaccination. No background risk is assumed for TTS.

Observed risk events
The observed events after vaccination are recorded by EudraVigilance by vaccine, age and gender. In our analysis we have used the dataset dd. 13 October 2021 for Myocarditis and 25 July 2021 for TTS.

Sensitivity analysis
Given the variability in the estimation of the background incidence rate of Myocarditis and missing information, a sensitivity analysis is performed by repeating the Observed-Expected ratio risk assessment for each data source separately and pooled via two weighting schemes. Additionally, the redistribution of the vaccine coverage is performed in two ways, with and without multiple imputation, where the seed for the multiple imputation is varied as a sensitivity analysis.

6.6 Benefit-risk Assessment Toolkit

The interactive dashboard for the benefit-risk contextualization of COVID-19 in the EU can be accessed via https://dsi-uhasselt.shinyapps.io/covid_vaccine_risks_and_benefits/ until May 2022. A username and password has been sent in a separate email to EMA. Other RStudio accounts can be given access on request. Source code for the toolkit will be provided to EMA for hosting the interactive dashboard internally.

The tool is implemented in a generic way to include information about new VoCs and specification of different age groups (harmonized with the specification of age groups for the risk side), at least if the input data is formatted in the correct way. Moreover, the inclusion of new vaccines is possible upon specification of parameters governing the vaccine properties in the context of the different VoCs. The inclusion of additional booster vaccinations is not included in the tool. The tool allows for any upcoming safety signal of the vaccines (including potentially new vaccines), with any corresponding risk specific age group (harmonized with the benefit input data). Using the same tool for other diseases might be difficult since the structure of the disease (and the parameters used to calculate the benefits; e.g., vaccine efficacy, waning effect, etc) will be different.

7 Results

In this section, we provide results of the **benefit-risk analysis** based on the methodology described above. First, we focus on the quantification of benefits with regard to COVID-19 vaccination after which risk assessments are provided. Finally, results concerning risks and benefits are combined.

7.1 Benefit Quantification

The benefits of vaccination with different COVID-19 vaccines, estimated using the probabilistic model (PM; Section 6.1) given the infection dynamics present within the specific time interval, can be expressed in terms of the number of prevented confirmed COVID-19 cases, hospitalizations, ICU admissions, and COVID-19 related deaths (see Figure 3). Based on the default model parameters, an estimated total of 13,322,567 confirmed COVID-19 cases have been prevented with mRNA and adeno-based vaccines since the start of the COVID-19 vaccination program in the different European countries. Moreover, 933,230 COVID-19 hospitalizations are prevented and a total of 150,106 ICU admissions were averted as well. Finally, COVID-19 vaccination prevented an estimated 220,880 COVID-19 related deaths.

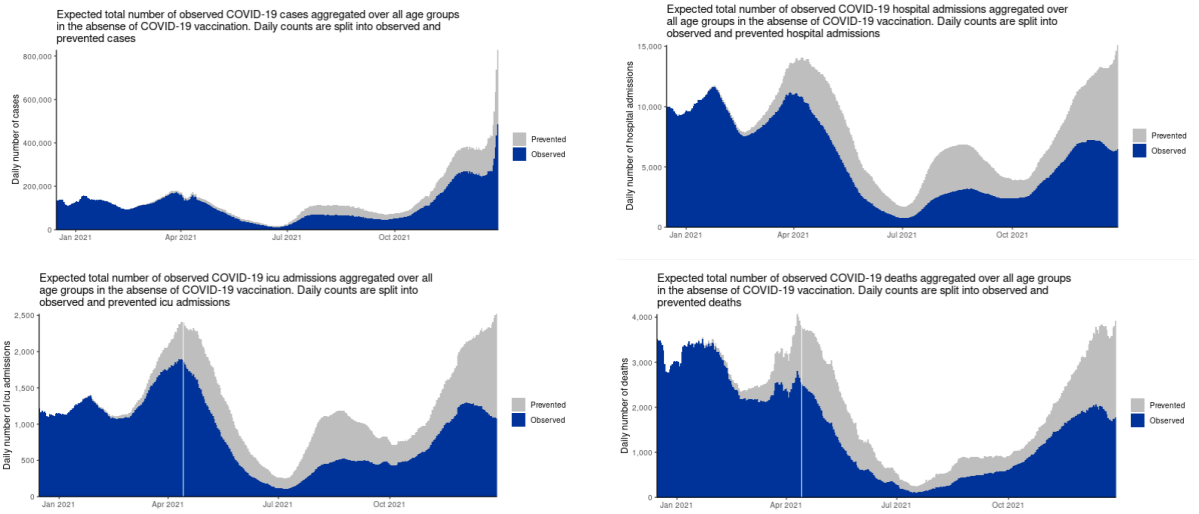

Figure 3: Weekly number of observed (blue) and predicted prevented (gray) confirmed cases *(top left)*, hospitalizations *(top right)*, ICU admissions *(bottom left)*, and deaths *(bottom right)* caused by SARS-CoV-2 infection and corresponding COVID-19 disease

Expressing the expected number of prevented events per 100,000 vaccinated individuals in each respective age category, allows for a direct comparison of the impact of vaccination among different age groups. For example, when comparing the benefits induced by the Comirnaty, Spikevax and Vaxzevria vaccine, between December 13, 2020 and December 31, 2021, we observe the largest reduction in the number of COVID-19 related hospitalizations and COVID-19 related deaths in the age group 80+, while the highest number of avoided ICU admissions was observed for the 70-79-year-old age group (see Figure 4–6).The number of prevented COVID-19 confirmed cases is high for all vaccines between 20-59 years and for the mRNA vaccines also in the age group 80+.

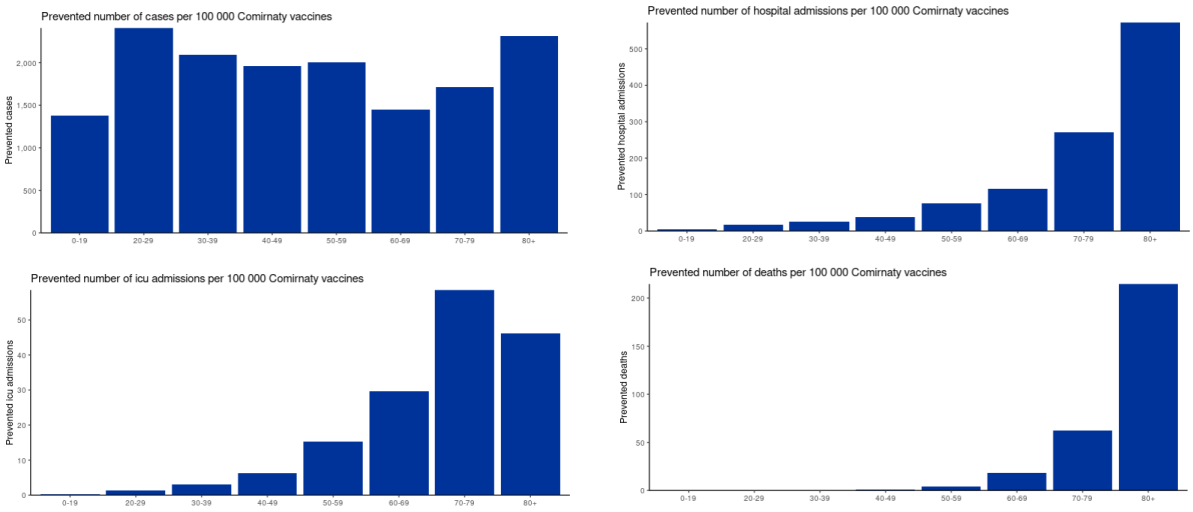

Figure 4: Expected number of prevented COVID-19 cases (top left), hospitalizations (top right), ICU admissions (bottom left), and mortality (bottom right) between December 13, 2020 and December 31, 2021 when 100,000 individuals would have been vaccinated with Comirnaty in the respective age categories

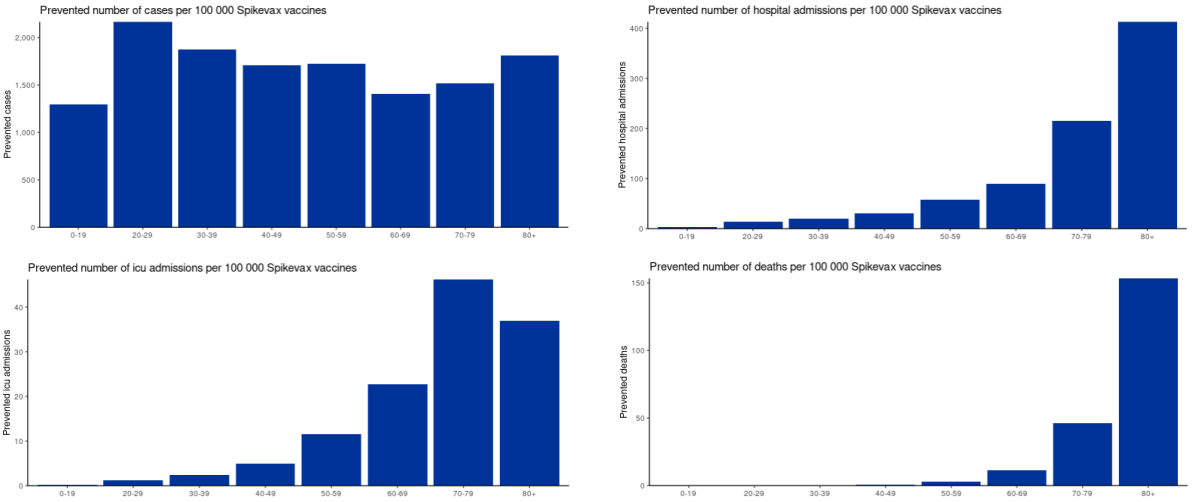

Figure 5: Expected number of prevented COVID-19 cases (top left), hospitalizations (top right), ICU admissions (bottom left), and mortality (bottom right) between December 13, 2020 and December 31, 2021 when 100,000 individuals would have been vaccinated with Spikevax in the respective age categories

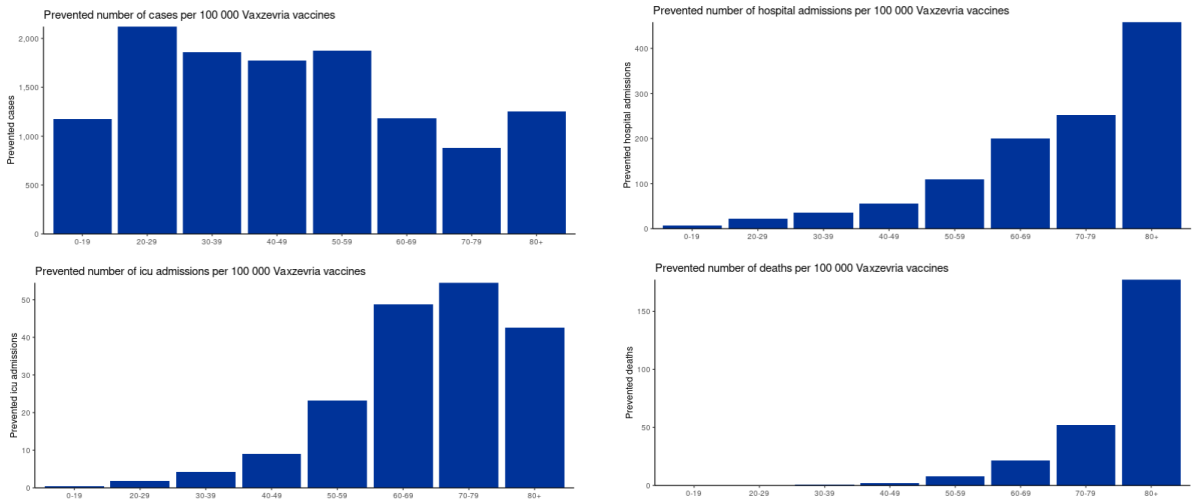

Figure 6: Expected number of prevented COVID-19 cases (top left), hospitalizations (top right), ICU admissions (bottom left), and mortality (bottom right) between December 13, 2020 and December 31, 2021 when 100,000 individuals would have been vaccinated with Vaxzevria in the respective age categories

7.2 Myocarditis and Pericarditis Risk of mRNA Vaccines

Observed cases

On 13 October 2021, 4635 myocarditis and pericarditis events related to the mRNA vaccines have been reported to EudraVigilance, of which 139 cases have missing age and/or gender information (24 missing gender, 111 missing age and 4 missing both gender and age). After redistribution of cases with the missing information over the observed age and gender distribution from the EudraVigilance reported cases with complete information, we observed that for most age categories and for both vaccines, there are more myocarditis events reported in males than in females (Table 3). On 25 July 2021, 503 TTS events within 30 days after Vaxzevria vaccination have been reported to EudraVigilance, of which 20 cases have missing age and/or gender information (19 missing age and 1 missing gender). After redistribution of cases with the missing information over the observed age and gender distribution from the EudraVigilance reported cases with complete information, we observed that for most age categories, there are more TTS events reported in females then in males (Table 3).

Table 3: EudraVigilance reported cases by gender, age group and vaccine type for Myocarditis dd. 13 October 2021 and TTS dd. 25 July 2021.

Myocarditis					TTS		
Age group	Comirnaty		Spikevax		Age group	Vaxzevria	
	Female	Male	Female	Male		Female	Male
12-17	69	302	0	32			
18-24	140	560	58	288	10-19	2	2
25-29	117	263	33	128	20-29	21	18
30-39	254	388	43	145	30-39	41	29
40-49	242	317	33	66	40-49	56	25
50-59	234	243	38	48	50-59	60	26
60-69	117	136	18	23	60-69	100	60
70-79	82	95	18	13	70-79	32	17
80+	37	48	4	2	80+	9	5

Background incidence rates

As TTS is only associated with vaccination [33], there are no background incidences rates for TTS. For myocarditis and pericarditis we dispose of background incidence rates, i.e., cases/100,000 person years, from 3 databases:

- Agenzia regionale di sanità della Toscana (ARS) Database (primary and secondary care) (January 2020 - June 2021);
- BIFAP Program: A data resource for Pharmacoepidemiological research in Spain (primary care) (January 2020 - August 2021)
  - BIFAP_PCHOSP
  - BIFAP_PCCOVID

In these datasets, the following information is available:

- Gender
- Age categories (0–4; 5–11; 12–17; 18–24; 25–29; 30–39; 40–49; 50–59; 60–69; 70–79; 80+)
- Three cohorts:
  - Pre-COVID-19 pandemic period (2017, 2018, 2019)
  - COVID-19 pandemic period - prior to introduction of vaccination in the age groups of interest
  - COVID-19 pandemic period - after introduction of vaccination in the age groups of interest

We can use each of these data sources for the background incidence rates separately. Unfortunately, in most data sources there are age-gender categories with no incidence rate (Table 4 and 5). In order to obtain an incidence rate for each age gender category we pool the incidence rates over each data source in each age gender category by inverse variance weighting. As there is a higher chance that a myocarditis diagnosis is made in secondary care as opposed to in primary care, there is a risk of under-reporting in primary care records (BIFAP). The ARS data source incorporates outcomes from both primary and secondary care, offering the option to verify this hypothesis to a certain extent. Indeed, the variability in IR between the data sources is large in most age-gender categories, as evidenced by highly significant Chi-squared tests for homogeneity and an I^2 close to 100% for each age gender category. The IR is in most categories lower in the BIFAP data sources then in the ARS data source (Table 4 and 5). Therefore, we choose to weight the IR estimates from the ARS data source additionally 10 times as much as the estimates from each of the BIFAP data sources.

For both the inverse variance weighting or when weighting additionally the ARS data source 10 times more than each of the BIFAP data sources, the pooled estimates of the IR per gender and age show a higher IR for males in all age categories in the period before COVID-19 and during COVID-19 prior to vaccination (Figures 7 and 8 and Table 4 and 5). This age difference is less pronounced in the period during the COVID-19 pandemic prior to vaccination.

When given more weight to the ARS data source, the IR is higher for most of the age categories. This follows from the higher IR in the ARS data source, that includes both primary and secondary care, compared to the lower IR in the BIFAP data sources, which include only primary care information (Figures 7 and 8 and Table 4 and 5).

Strikingly, the IR is much higher in the period during COVID-19 than before the pandemic, which may be a true effect or a consequence of the uncertainty around the estimation due to the smaller person years in the period during COVID-19 (Figures 7 and 8 and Table 4 and 5). Nonetheless, as COVID-19 can also cause myocarditis, the myocarditis risk of vaccination should be compared to the period during COVID-19, before vaccination started.

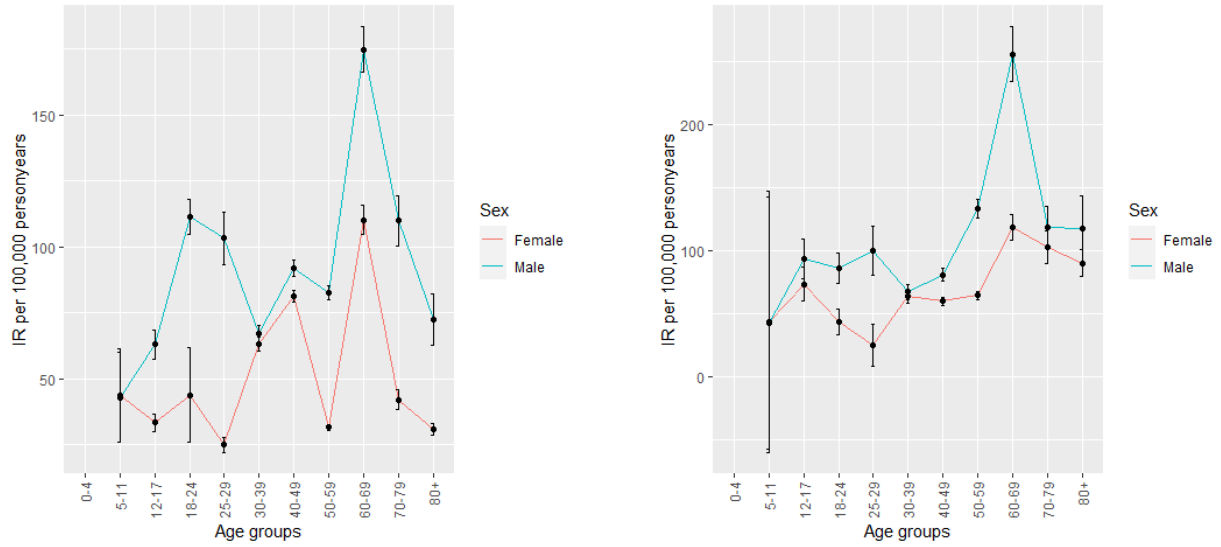

Figure 7: Pooled myocarditis background rate **during COVID-19 prior to vaccination** per age group and sex, when including only inverse variance weighting (left) or when additionally including weights 1 for ARS and 0.1 for both BIFAP data sources (right)

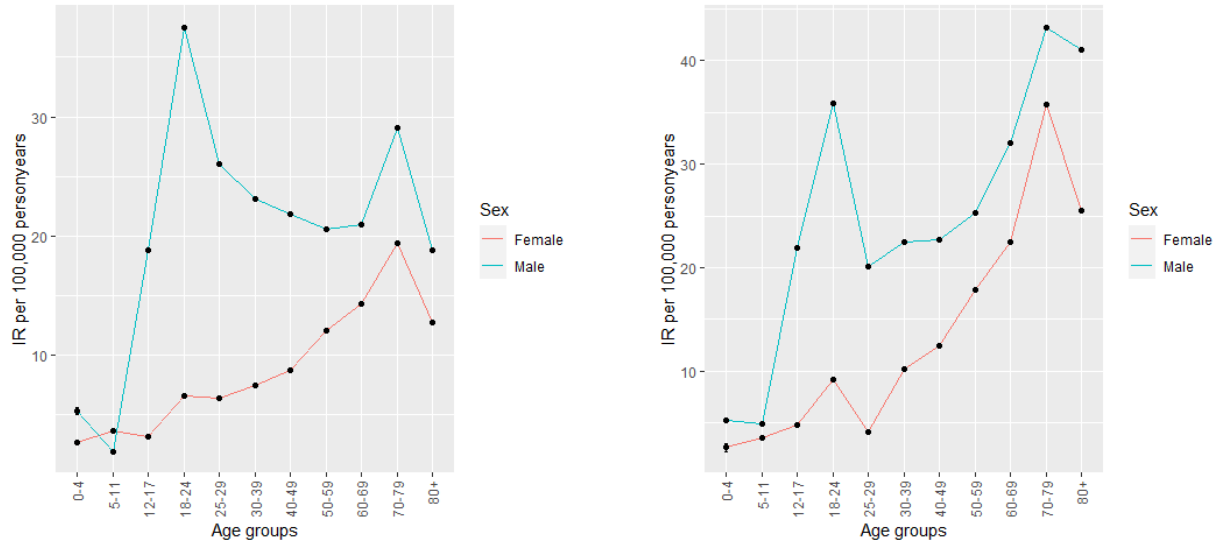

Figure 8: Pooled myocarditis background rate **before COVID-19** per age group and sex, when including only inverse variance weighting (left) or when additionally including weights 1 for ARS and 0.1 for both BIFAP data sources (right)

Table 4: Myocarditis background incidence rate, IR (variance), **during COVID-19 prior to vaccination** per gender and age group for the pooled and single data sources

Age	Pool 1/0.1/0.1	Pool 0.1/0.1/0.1	ARS	BIFAP_HOSP	BIFAP_COVID
			Female		
5-11	43.71(52.83)	43.71(9.06)	0	0	43.71 (5.23)
12-17	73.84(6.96)	33.29(1.64)	182.65 (22.83)	0	26.84 (0.99)
18-24	43.85(5.32)	43.85(9.12)	43.85 (5.26)	0	0
25-29	24.98(8.63)	24.98(1.48)	0	0	24.98 (0.85)
30-39	64.18(2.71)	63.13(1.26)	64.79 (3.83)	62.22 (10.60)	62.79 (0.98)
40-49	60.31(1.69)	81.28(1.21)	53.73 (1.98)	266.95 (32.52)	90.52 (1.12)
50-59	64.74(1.74)	31.5(0.52)	109.43 (3.64)	0	24.48 (0.33)
60-69	118.72(5.26)	110.24(2.85)	122.65 (6.86)	200.69 (36.76)	100.42 (2.3)
70-79	103.11(6.59)	41.95(1.91)	191.93 (14.4)	0	29.53 (1.19)
80+	90.38(5.48)	30.67(1.15)	354.99 (26.54)	0	22.33 (0.68)
			Male		
5-11	42.98(51.08)	42.98(8.76)	0	0	42.98 (5.06)
12-17	93.96(7.99)	62.97(2.76)	124.45 (14.13)	137.4 (51.69)	52.18 (1.37)
18-24	86.56(6.1)	111.48(3.43)	75.61 (7.83)	331.39 (100.22)	117.98 (2.72)
25-29	99.94(9.87)	103.33(5.07)	98.24 (13.21)	0	104.78 (3.76)
30-39	67.54(3.08)	67.09(1.53)	67.77 (4.19)	74.81 (15.32)	66.29 (1.20)
40-49	81.02(2.58)	91.94(1.55)	76.66 (3.22)	371.27 (53.91)	91.39 (1.27)
50-59	133.42(3.69)	82.73(1.39)	176.06 (6.06)	55.27 (8.36)	70.17 (1.04)
60-69	256.28(11.05)	174.71(4.4)	318.02 (17.31)	214.34 (41.93)	145.15 (3.20)
70-79	119.09(8.2)	109.87(4.8)	122.91 (10.34)	114.36 (35.81)	104.01 (4.23)
80+	117.55(13.5)	72.25(4.95)	157.26 (22.57)	0	59.91 (3.28)

Table 5: Myocarditis background incidence rate, IR (variance), **before COVID-19** per gender and age group for the pooled and single data sources

Age	Pool 1/0.1/0.1	Pool 0.1/0.1/0.1	ARS	BIFAP_HOSP	BIFAP_COVID
			Female		
5-11	3.62(0.02)	3.62(0.03)	3.62 (0.02)	0.00	0.00
12-17	4.82(0.01)	3.17(0.01)	5.78 (0.02)	0.00	2.56 (0.01)
18-24	9.2(0.02)	6.58(0.01)	11.38 (0.03)	4.83 (0.02)	6.15 (0.01)
25-29	4.2(0.01)	6.42(0.01)	11.39 (0.01)	10.63 (0.06)	8.3 (0.01)
30-39	10.19(0.01)	7.47(0.01)	11.40 (0.02)	8.77 (0.02)	6.16 (0.01)
40-49	12.49(0.01)	8.77(0.01)	11.41 (0.01)	9.51 (0.01)	7.06 (0.01)
50-59	17.88(0.01)	12.12(0.01)	11.42 (0.02)	11.18 (0.02)	9.65 (0.01)
60-69	22.45(0.02)	14.32(0.01)	11.43 (0.02)	13.58 (0.02)	11.01 (0.01)
70-79	35.73(0.03)	19.37(0.01)	11.44 (0.05)	18.02 (0.04)	13.6 (0.01)
80+	25.46(0.02)	12.76(0.01)	11.45 (0.04)	13.03 (0.03)	8.76 (0.01)
			Male		
5-11	4.98(0.02)	1.94(0.01)	8.47 (0.04)	0.00	1.24 (0.01)
12-17	21.89(0.04)	18.83(0.02)	23.31 (0.06)	21.52 (0.10)	16.51 (0.02)
18-24	35.85(0.07)	37.48(0.04)	35.13 (0.09)	47.11 (0.20)	36.63 (0.04)
25-29	20.07(0.05)	26.03(0.04)	18.27 (0.06)	38.58 (0.21)	29.06 (0.04)
30-39	22.51(0.02)	23.1(0.01)	22.27 (0.03)	27.11 (0.06)	22.63 (0.01)
40-49	22.7(0.02)	21.8(0.01)	23.08 (0.02)	29.79 (0.05)	19.86 (0.01)
50-59	25.33(0.02)	20.6(0.01)	27.53 (0.02)	22.34 (0.04)	17.55 (0.01)
60-69	31.98(0.03)	21.01(0.01)	39.21 (0.04)	20.65 (0.04)	16.45 (0.01)
70-79	43.15(0.04)	29.12(0.02)	50.85 (0.06)	22.12 (0.06)	24.15 (0.02)
80+	41.05(0.06)	18.85(0.02)	67.46 (0.12)	24.96 (0.09)	12.01 (0.01)

Vaccine coverage

As described in Section 6.4.1, two data sources are available with vaccine coverage data, from ECDC and via the Member States directly. To which date the vaccine coverage data is used to estimate the expected risk events, depends on the date of the Eudravigilance report and the time window after vaccination in which the risk events are evaluated. As for myocarditis, the Eudravigilance report dates from 13 October 2021 and events are evaluated in a time window 14 days after vaccination, the vaccine coverage up week 39, which ends with 3 October, is considered. As there is no background incidence rate for TTS, the expected risk is zero and no vaccine coverage is required for TTS.

The vaccine coverage in the ECDC data with missing gender and/or age information is distributed via two methodologies, with fixed proportions and with uncertainty around the proportions via multiple imputation. When redistributing with fixed proportions, the age proportions in the ECDC coverage data is used and the gender proportions of the Member States data. When redistributing with multiple imputation, the age and gender proportions from the Member States data is used. Thus, the analysis with fixed proportions and with multiple imputation differ, besides the uncertainty in proportions, also in the estimated age proportions. For most age categories the estimated age proportions are very similar between both data sources

(Table 6). Note that the ECDC data is based on 17 countries, while the Member States data is based on 19 countries, which explains the larger total vaccine coverage for the latter, despite being of an earlier date.

Although for the mRNA vaccines a few countries (Finland, Croatia, Latvia and Slovenia) have not reported the coverage in the lowest age categories < 12 years in the Member States data, this missing information is for the current analysis irrelevant since myocarditis events reported to Eudravigilance are only ≥ 12 years.

Table 6: Age proportions in the vaccine coverage data of ECDC (dd. 3 October 2021) and the vaccine coverage data requested to the Member States (dd. 30 September 2021). * Note that the ECDC data joins to a 10–17 years age category, while the Member States data joins to a 12–17 years age category

Age	Coverage ECDC	Coverage Member States	Proportion ECDC	Proportion Member States
		Comirnaty		
12-17*	9,764,639	16,166,683	6.31	6.89
18-24	10,849,597	19,259,722	7.01	8.21
25-49	56,124,325	86,002,046	36.27	36.65
50-59	26,525,178	38,713,353	17.14	16.50
60-69	17,259,724	26,161,510	11.15	11.15
70-79	20,447,341	28,428,720	13.21	12.11
80+	13,775,447	19,930,817	8.90	8.49
Total	154,746,251	234,662,851	100	100
		Spikevax		
12-17*	847,873	1,019,211	3.69	3.00
18-24	2,357,673	3,485,431	10.26	10.27
25-49	9,639,186	14,368,747	41.95	42.33
50-59	4,197,445	6,537,764	18.27	19.26
60-69	2,483,233	3,590,475	10.81	10.58
70-79	2,218,530	3,091,825	9.66	9.11
80+	1,233,000	1,854,849	5.37	5.46
Total	22,976,940	33,948,302	100	100

When comparing the vaccine coverage after redistribution with 20 imputations with the Member States age category proportions and the redistribution with the fixed ECDC age category proportions, the vaccine coverage is fairly comparable between the two methods of redistribution, except for the lowest age categories where the coverage is smaller in the fixed ECDC age categories redistribution for both vaccines (Table 7).

Table 7: Vaccine Coverage by vaccine, age and gender category for the redistribution of coverage with missing age and gender by the ECDC or Member States age category proportions. For the Member States redistribution the mean coverage over 20 imputed data sets is displayed per category

	Comirnaty		Spikevax	
Age	Coverage ECDC age redistribution	Coverage Member States age redistribution	Coverage ECDC age redistribution	Coverage Member States age redistribution
		Female		
5-11	104,083	117,305	3,680	5,742
12-17	13,243,196	13,796,430	1,002,159	929,080
18-24	16,006,005	17,264,318	3,165,681	3,165,356
25-29	12,589,761	12,726,604	2,451,820	2,448,361
30-39	29,742,352	30,094,757	5,311,917	5,274,864
40-49	35,982,787	36,267,593	5,166,444	5,186,605
50-59	37,743,450	37,238,302	5,415,672	5,498,707
60-69	26,410,465	26,395,991	3,501,660	3,470,054
70-79	28,859,186	27,826,975	3,137,415	3,076,472
80+	24,137,397	23,662,786	2,285,725	2,281,345
		Male		
5-11	110,316	113,842	3,839	8,171
12-17	13,748,904	14,265,756	1,055,850	978,715
18-24	15,222,017	16,387,052	3,073,857	3,055,890
25-29	12,315,457	12,329,206	2,391,135	2,444,385
30-39	28,909,659	29,067,126	5,184,071	5,196,293
40-49	35,001,383	35,194,886	5,120,939	5,079,689
50-59	36,560,865	36,199,017	5,534,111	5,657,565
60-69	23,651,868	23,655,648	3,209,625	3,179,167
70-79	24,614,881	23,647,170	2,657,074	2,600,371
80+	15,019,511	14,809,616	1,458,548	1,450,570

Observed-Expected ratio

The observed-expected ratios at 14 days can be obtained by formula (3):

$$R_{a,s} = \frac{EV_{a,s}100,000}{\mathsf{IR}_{a,s}n_{a,s}t},$$

where $EV_{a,s}$ is the corresponding age, gender and vaccine value from Table 3, $\mathsf{IR}_{a,s}$ the corresponding age and gender value from Table 4, $n_{a,s}$ the product of the corresponding age and gender value from Table 7 and $t = 14/365$, the time horizon in years. The variance of the observed-expected ratios is obtained as outlined in Section 6.4.2.

The observed-expected ratios at 14 days using the pooled background incidence rate during COVID-19 prior to vaccination, with both inverse variance weighting and additional $(1, 0.1, 0.1)$ weight and multiple imputation, show higher observed-expected ratios in the age categories < 40 years for both genders and

vaccine types (Figure 9 and Table 8). Only for Spikevax the observed-expected ratio is above 1, indicating a higher observed myocarditis risk than expected. More specifically, the risk is increased for males in age groups 18–24y and less so for 25–39y after Spikevax vaccination. In the age categories < 40y the risk of myocarditis after vaccination is slightly higher in males compared to females. The wide variability for females aged between 25–29 is explained by a zero IR estimate in 2 of the 3 background data sources (see right Figure 7). When comparing the O/E ratio between genders, the uncertainty of the point estimates of the O/E ratio should always be considered.

Weighting each of the three data sources equally does not alter the conclusions much (Table 8 and Figure 11). Using the fixed proportion redistribution and considering each background incidence rate data source individually does not change the conclusions either, except for the BIFAP HOSP data source, which does not show any increased risk (Table 8 and Figures 10–11). Interestingly, the multiple imputation redistribution method reduces the variance for the higher age categories, while it increases the uncertainty for the smaller age groups (Figure 11). Varying the seed for the multiple imputation does not alter the observed results (data not shown).

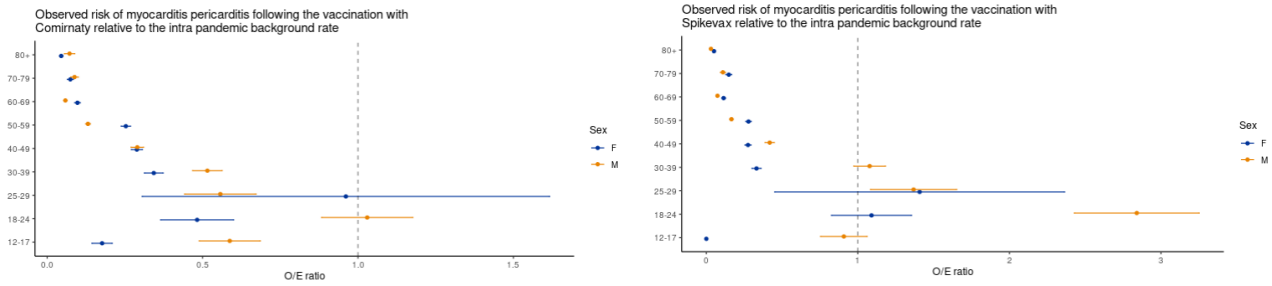

Figure 9: The Observed-Expected ratio per age, gender and vaccine type (left Comirnaty, right Spikevax), using the pooled background incidence rate **during COVID-19 prior to vaccination** with both inverse variance weight and additional (1,0.1,0.1) weight and multiple imputation

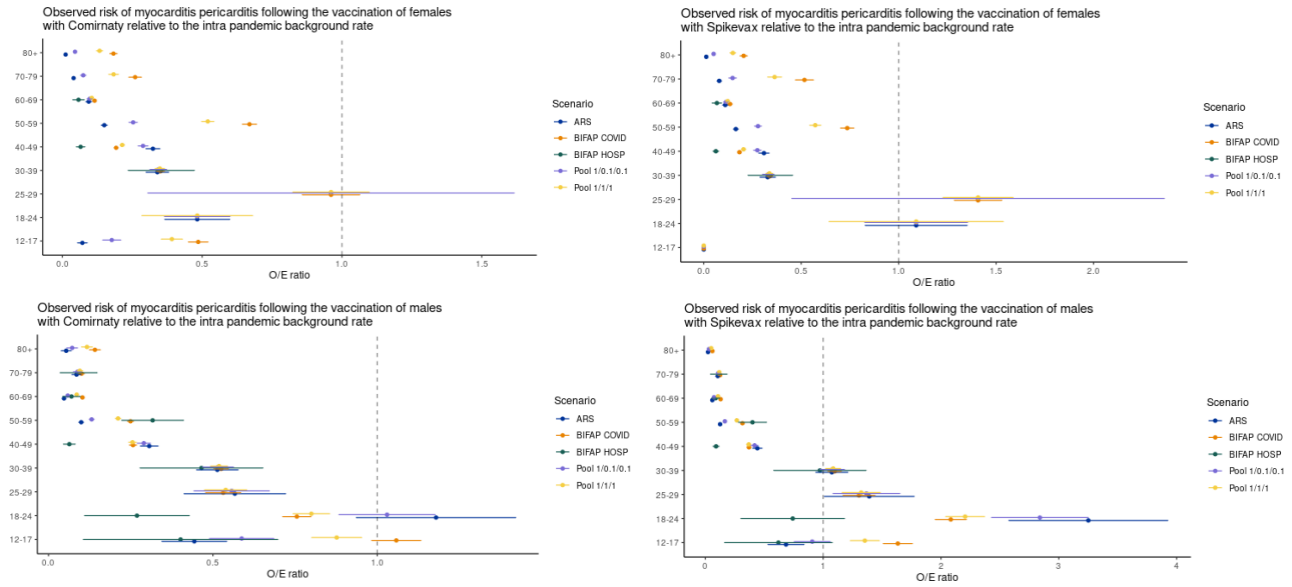

Figure 10: The observed-expected ratio per age, gender (top: Female; bottom: Male) and vaccine type (left: Comirnaty; right: Spikevax), using the incidence rate **during COVID-19 prior to vaccination** for several background rates and multiple imputation

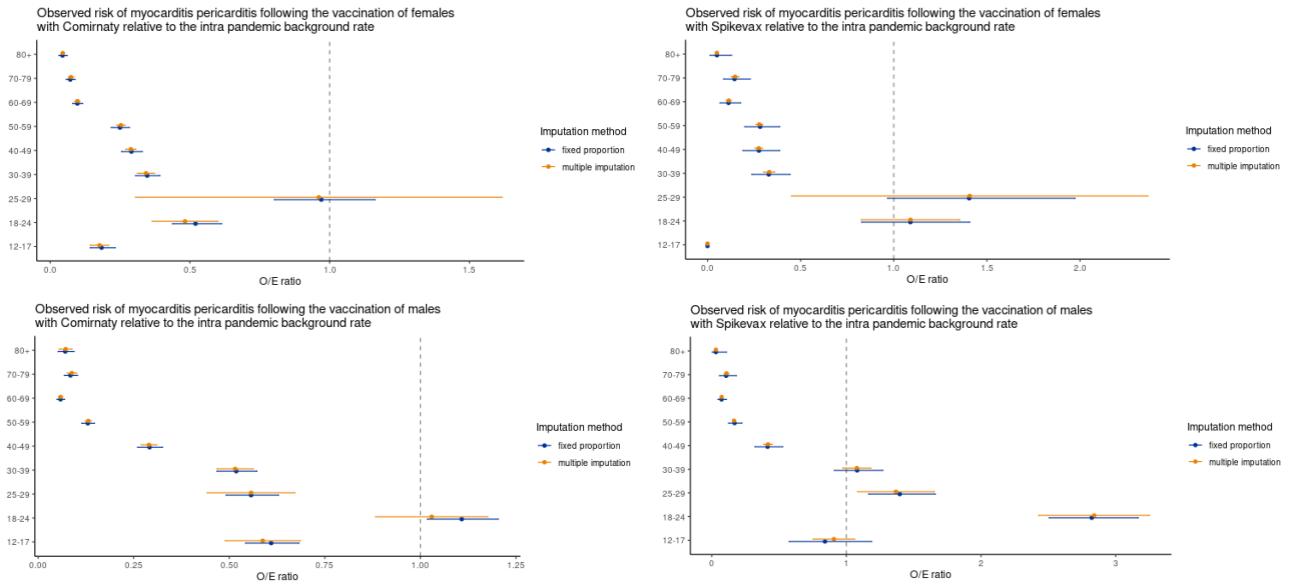

Figure 11: The observed-expected ratio per age, gender (top: Female; bottom: Male) and vaccine type (left: Comirnaty; right: Spikevax), using the pooled background incidence rate **during COVID-19 prior to vaccination** with both inverse variance weight and additional (1,0.1,0.1) weight comparing multiple imputation and fix proportion redistribution of the vaccine coverage

Table 8: Expected Myocarditis cases **during COVID-19 prior to vaccination** and Observed–Expected ratio for several background incidence rate data sources

Comirnaty											
		ARS		BIFAP HOSP		BIFAP COVID		Pool 0.1/0.1/0.1		Pool 1/0.1/0.1	
Age	Obs	Exp 14d	O/E (CI)	Exp 14d	O/E (CI)	Exp 14d	O/E (CI)	Exp 14d	O/E (CI)	Exp 14d	O/E (CI)
						Female					
12-17	69	1041	0.07(0.05-0.08)	0	0	153	0.45(0.42-0.49)	190	0.37(0.33-0.40)	421	0.17(0.13-0.20)
18-24	140	316	0.45(0.34-0.56)	0	0	0	0	316	0.45(0.27-0.64)	316	0.45(0.34-0.56)
25-29	117	0	0	0	0	133	0.88(0.80-0.96)	131	0.88(0.76-1.00)	131	0.88(0.28-1.48)
30-39	254	815	0.31(0.28-0.35)	782	0.33(0.22-0.44)	790	0.32(0.31-0.34)	794	0.32(0.30-0.34)	807	0.32(0.29-0.34)
40-49	242	833	0.30(0.28-0.32)	4138	0.06(0.05-0.07)	1403	0.18(0.17-0.18)	1260	0.20(0.19-0.20)	935	0.27(0.25-0.28)
50-59	234	1701	0.14(0.13-0.15)	0	0	381	0.62(0.59-0.64)	490	0.48(0.46-0.50)	1007	0.23(0.22-0.25)
60-69	117	1387	0.08(0.08-0.09)	2270	0.05(0.03-0.07)	1136	0.10(0.10-0.11)	1247	0.09(0.09-0.10)	1343	0.09(0.08-0.10)
70-79	82	2271	0.04(0.03-0.04)	0	0	349	0.23(0.21-0.25)	496	0.16(0.15-0.18)	1220	0.07(0.06-0.08)
80+	37	3397	0.01(0.01-0.01)	0	0	214	0.17(0.16-0.18)	294	0.12(0.11-0.13)	865	0.04(0.04-0.05)
						Male					
12-17	302	679	0.44(0.35-0.54)	750	0.40(0.11-0.70)	285	1.06(0.98-1.13)	344	0.88(0.80-0.95)	513	0.59(0.49-0.69)
18-24	560	476	1.2(0.94-1.42)	2088	0.27(0.11-0.43)	743	0.76(0.71-0.80)	701	0.80(0.74-0.86)	545	1.03(0.88-1.2)
25-29	263	472	0.57(0.41-0.72)	0	0	503	0.53(0.48-0.59)	497	0.54(0.47-0.60)	480	0.56(0.44-0.67)
30-39	388	750	0.51(0.45-0.58)	828	0.47(0.28-0.65)	733	0.53(0.50-0.55)	742	0.52(0.49-0.55)	747	0.52(0.47-0.56)
40-49	317	1007	0.31(0.28-0.33)	4879	0.06(0.05-0.08)	1201	0.26(0.25-0.27)	1208	0.26(0.24-0.27)	1065	0.29(0.27-0.31)
50-59	243	2448	0.10(0.09-0.11)	768	0.32(0.22-0.41)	975	0.25(0.24-0.26)	1150	0.21(0.20-0.22)	1855	0.13(0.12-0.14)
60-69	136	2886	0.05(0.04-0.05)	1945	0.07(0.04-0.10)	1317	0.10(0.10-0.11)	1585	0.09(0.08-0.09)	2325	0.06(0.05-0.06)
70-79	95	1117	0.09(0.07-0.10)	1040	0.09(0.04-0.15)	946	0.10(0.09-0.11)	999	0.10(0.09-0.10)	1083	0.09(0.08-0.10)
80+	48	875	0.05(0.04-0.07)	0	0	333	0.14(0.13-0.16)	402	0.12(0.10-0.13)	654	0.07(0.06-0.09)
Spikevax											
						Female					
12-17	0	65	0	0	0	10	0	12	0	26	0
18-24	58	55	1.09(0.83-1.358)	0	0	0	0	55	1.09(0.64-1.54)	55	1.09(0.83-1.35)
25-29	33	0	0	0	0	24	1.41(1.29-1.53)	24	1.41(1.23-1.59)	24	1.41(0.45-2.36)
30-39	43	132	0.32(0.29-0.37)	127	0.34(0.23-0.46)	128	0.34(0.32-0.36)	129	0.34(0.32-0.36)	131	0.33(0.30-0.36)
40-49	33	107	0.31(0.28-0.34)	530	0.06(0.05-0.08)	180	0.18(0.17-0.19)	161	0.20(0.19-0.22)	120	0.28(0.26-0.30)
50-59	38	227	0.17(0.15-0.18)	0	0	51	0.74(0.70-0.77)	65	0.57(0.54-0.60)	134	0.28(0.26-0.30)
60-69	18	168	0.1(0.10-0.13)	275	0.07(0.04-0.09)	138	0.14(0.12-0.15)	151	0.12(0.11-0.13)	163	0.11(0.10-0.13)
70-79	18	224	0.08(0.06-0.09)	0	0	35	0.52(0.47-0.56)	49	0.36(0.33-0.40)	121	0.15(0.13-0.17)
80+	4	323	0.01(0.01-0.02)	0	0	20	0.21(0.19-0.22)	28	0.15(0.13-0.16)	82	0.05(0.04-0.06)
						Male					
12-17	32	47	0.69(0.53-0.84)	52	0.62(0.16-1.08)	20	1.63(1.51-1.76)	24	1.35(1.23-1.48)	35	0.91(0.75-1.06)
18-24	288	88	3.25(2.58-3.9)	388	0.74(0.30-1.18)	138	2.08(1.95-2.22)	130	2.21(2.04-2.37)	101	2.84(2.43-3.25)
25-29	128	94	1.39(1.01-1.77)	0	0	100	1.31(1.17-1.44)	99	1.32(1.16-1.49)	96	1.37(1.08-1.65)
30-39	145	135	1.07(0.94-1.21)	149	0.97(0.58-1.37)	132	1.10(1.04-1.16)	134	1.09(1.02-1.15)	135	1.08(0.97-1.18)
40-49	66	147	0.44(0.40-0.48)	711	0.09(0.07-0.12)	175	0.37(0.35-0.39)	176	0.37(0.35-0.39)	155	0.42(0.39-0.45)
50-59	48	391	0.13(0.12-0.14)	123	0.40(0.28-0.52)	156	0.32(0.30-0.33)	184	0.27(0.25-0.28)	296	0.17(0.16-0.18)
60-69	23	379	0.06(0.05-0.07)	256	0.09(0.05-0.12)	173	0.13(0.12-0.14)	208	0.11(0.10-0.12)	306	0.07(0.07-0.08)
70-79	13	120	0.11(0.09-0.13)	111	0.11(0.04-0.19)	101	0.13(0.11-0.14)	107	0.12(0.11-0.13)	116	0.11(0.09-0.13)
80+	2	77	0.02(0.02-0.03)	0	0	29	0.06(0.05-0.07)	35	0.05(0.04-0.06)	57	0.03(0.02-0.04)

As the background incidence rates are much lower in the period before the COVID-19 pandemic, the Observed–Expected ratios are higher when compared to the ratios during COVID-19 prior to vaccination (Figure 12). The Observed–Expected ratio for Spikevax is again higher than for Comirnaty. The risk of myocarditis is increased in age categories <50y of age, for both genders. The highest risks are observed between 18–29 years. Weighting each of the three data sources equally, or comparing each data source individually do not change the conclusions much (Figure 11).

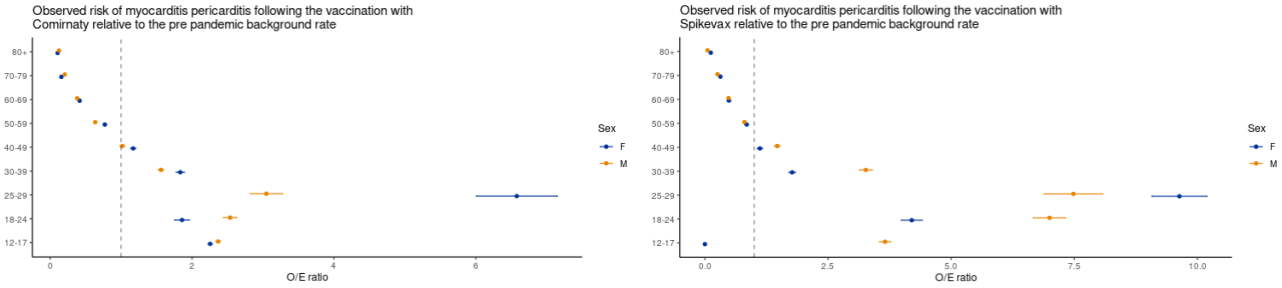

Figure 12: The Observed-Expected ratio per age, gender and vaccine type (left Comirnaty, right Spikevax), using the pooled background incidence rate **before COVID-19** with both inverse variance weight and manual (1,0.1,0.1) weight

7.3 Benefit-Risk of Myocarditis and TTS

Setting the benefits, in terms of prevented hospitalization, ICU admission and mortality, off against the difference in observed versus expected myocarditis risk after vaccination with Cominarty, the highest number of prevented hospitalizations, ICU admissions and deaths occur in the 80+ age group, whereas the expected risks are highest in the 18–24 age group (Note that the scale of the x-axis is different for each age group) (Figure 13). The expected risks in age groups > 40 years clearly outweigh the benefits induced by COVID-19 vaccination. While there is an increased risk < 40 years, vaccination in these age groups prevent substantially hospitalizations due to COVID-19. The severity of the myocarditis events should also be balanced against severe clinical events, such as ICU admission and deaths due to COVID-19 (Figure 13).

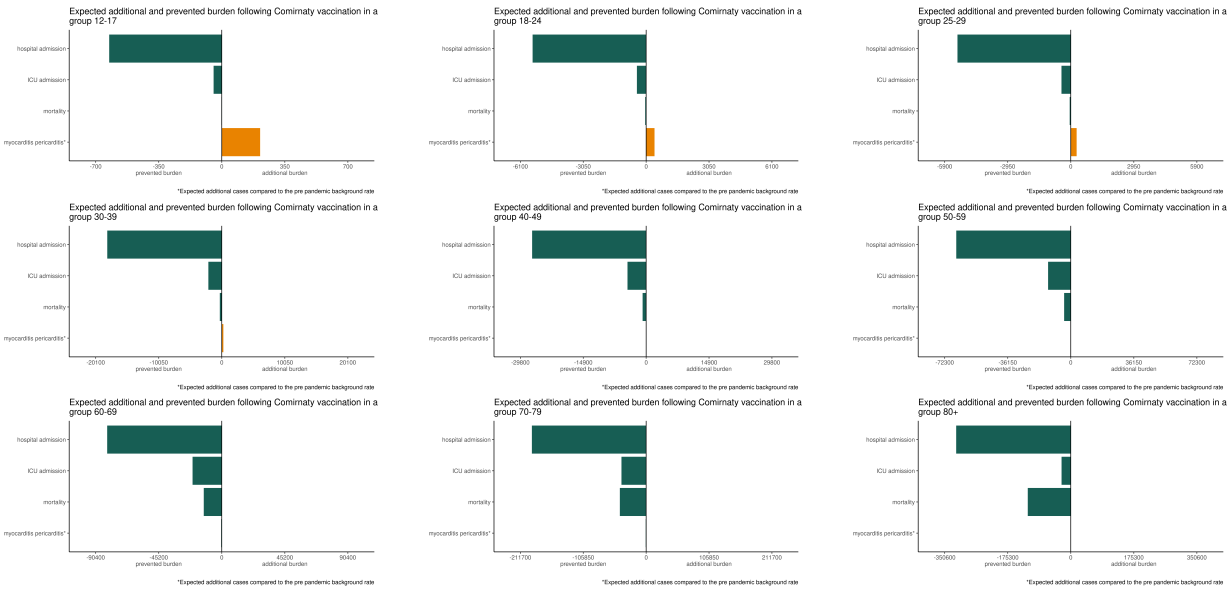

Figure 13: Comparison of the benefits and risks (myocarditis pericarditis) associated with two doses of *Cominarty* COVID-19 vaccine per age catgeories.

Similarly, vaccination with Spikevax leads to a clear benefit of vaccination in > 40 year age group with no increased risk of myocarditis (Figure 14). Although it is less clear due to the different scale of the x-axis for each sub-image, there is a larger myocarditis burden for Spikevax compared to Comirnaty. Again, the increased burden should be carefully evaluated against the prevented burden due to COVID-19 and its severity.

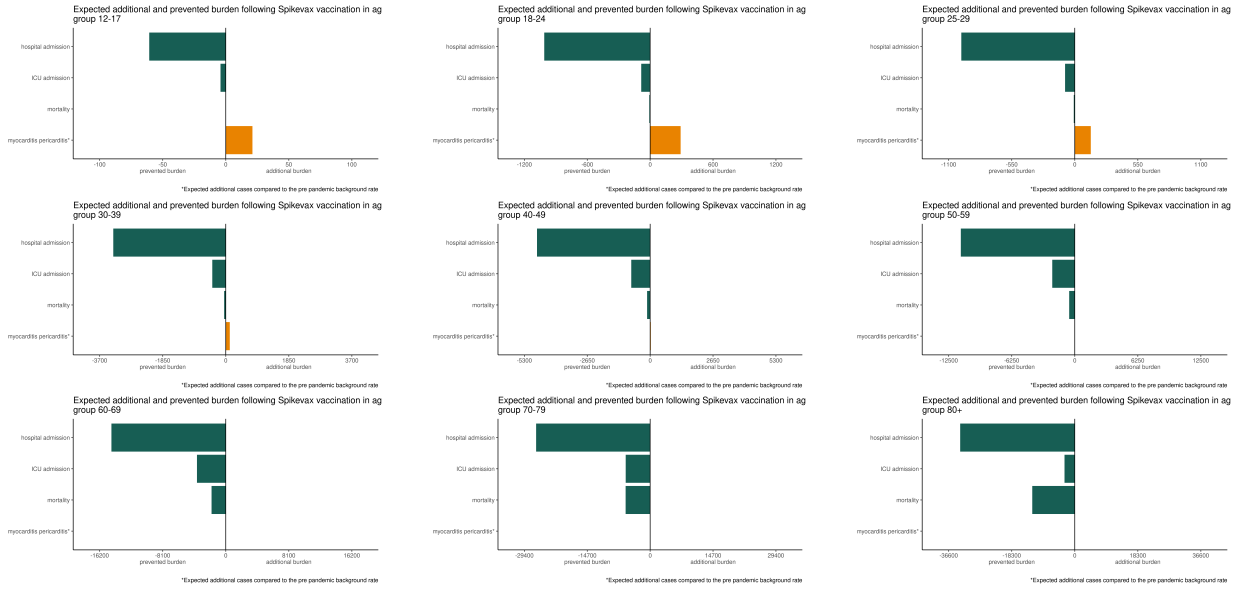

Figure 14: Comparison of the benefits and risks (myocarditis pericarditis) associated with two doses of *Spikevax* COVID-19 vaccine per age category.

Finally, setting the benefits of Vaxzevria vaccination against the difference in observed versus the expected TTS risks, again the benefits clearly outweigh the risks (Figure 15). The number of prevented hospitalizations, ICU admissions, and deaths, as well as the risks of TTS are highest in the 60-69-year-old age category. Note that the scales for risks and benefits in each age group are different.

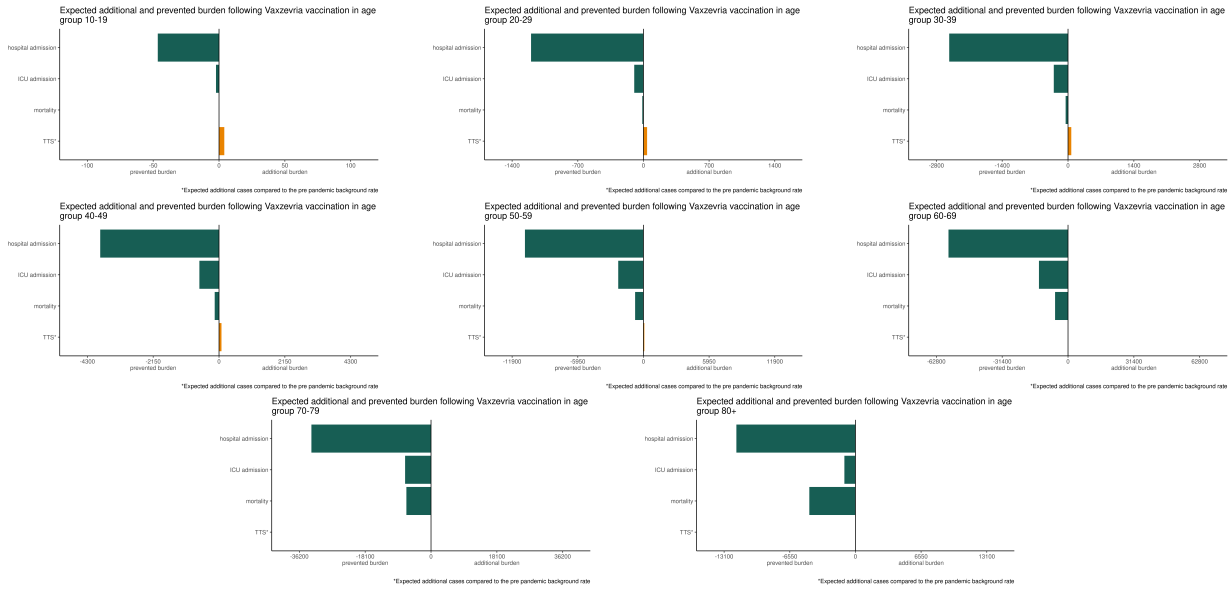

Figure 15: Comparison of the benefits and risks (TTS) associated with two doses of *Vaxzevria* COVID-19 vaccine per age category.

8 Feasibility of Benefit-Risk Composite Measure

During the last decade, quantitative benefit-risk assessment has been the subject of identification, classification and development of recommendations by several large initiatives within and outside Europe [34, 35]. In 2009, two initiatives started in Europe with the aim to provide recommendations for quantitative benefit-risk assessment: (1) The Benefit–Risk Methodology Project led by the EMA [36, 37] and (2) the Pharmacoepidemiological Research on Outcomes of Therapeutics (PROTECT) consortium [38]. The Center for Innovation in Regulatory Science (CIRS) started in 2012 the Unified Methodologies for Benefit–Risk Assessment (UMBRA) project of which guidelines are currently in use by Canada, Australia, Switzerland and Singapore [39].

Following these first initiatives, the International Society for Pharmacoeconomics and Outcomes Research (ISPOR) Risk–Benefit Management Working Group developed promising general quantitative benefit-risk assessment methods further [40, 41, 42], while the IMI-ADVANCE (Innovative Medicines Initiative - Accelerated Development of Vaccine Benefit–Risk) project revisited between 2013-2019 all methodologies described in the systematic reviews of PROTECT and ISPOR and evaluated their suitability specifically focusing on benefit-risk assessment in the context of vaccines [43, 44].

Both the general initiatives as well as the vaccine-specific IMI-ADVANCE project identified Multi Criteria Decision Analysis (MCDA) and Stochastic Multi criteria Acceptability Analysis (SMAA) as the most promising methods for conducting quantitative benefit-risk assessments.

MCDA is an umbrella term, finding its origin in decision theory, which covers a large variety of methods to inform decision making based on multiple criteria. It is broadly applicable to decision making, and thus

also to drug benefit-risk analysis and consists of identifying important criteria for the decision making and subsequently combining these criteria via a weighted regression approach into a value judgment [45, 41, 46]. The regression method combines the weighted criteria either additively, via a linear or non-linear value function, or multiplicatively. Numerous methods for assigning weights or preference elicitation exist, such as direct weighting, Simple Multi Attribute Rating Technique, pairwise comparison, swing-weighting, and decompositional methods, among others, which can be obtained from focus groups, experts or surveys [45, 41, 46]. However, obtaining these weights is often not straightforward and panellists may find it difficult to understand how to apply a more complex preference elicitation algorithm. Recently, in a vaccine specific MCDA simulation study, participants found one of these more complex preference elicitation algorithms, more specifically swing-weighting, difficult to understand, even after a face-to-face training session on preference elicitation and after practicing MCDA swing-weighting using specialized software [47]. This was especially the case when non-linear value functions were selected [47].

When it is difficult to obtain such preferences or when priorities are conflicting with regard to the assignments of weights, these weights can be replaced by ranks in MCDA (AHP [48] and MACBETH [49]) or weights can be defined as a stochastic value in SMAA, which accommodates statistical uncertainty with respect to the aforementioned weights [50, 51].

The Incremental Net Health Benefit (INHB) and Incremental Benefit-Risk Ratio (IBRR), two benefit-risk measures often used in the context of cost-effectiveness assessments (see, e.g. [52]), can be considered as an MCDA model [47]. It is indeed straightforward to see that the INHB is an MCDA model with an additive linear value function, since it sums, possibly weighted, differences between benefits and risks in the untreated and treated population. In the context of vaccines

$$\text{INHB} = \sum_{i=1}^{k} w_i(E_{0i} - E_{vi}) + \sum_{j=1}^{l} w_j(R_{0j} - R_{vj}),$$

with k and l the number of benefit and risk outcomes, respectively, E_0 the benefits before and E_v after vaccination, and similarly for the risks (R_0 and R_v, respectively). The weights w_i and w_j are all positive and reflect the relative severity of the health outcomes. If all weights are set to 1, all benefit and risk outcomes are considered equally important in the assessment.

Benefits and risks are often expressed in QALYs or derivations thereof [53], which are (currently) not readily available for COVID-19 vaccines. Recently, in a simulation study on rota-virus vaccination, benefits and risks were expressed as incidence rates [47], which are also available for COVID-19 vaccines.

However, the existing benefit-risk assessment methods have several disadvantages:

1. The advantages or disadvantages of vaccination are not clearly available from the INHB value, as the value will be continuous, unbounded and it depends on the number of events or risks, especially in comparison with vaccines having a different number of events.

2. MCDA with an additive linear value function such as the INHB, requires non-overlapping benefits and risks. Overlapping events will be counted multiple times due to the additive nature of the INHB. For example, the possible benefit of COVID-19 vaccination on COVID-19 related mortality will be counted multiple times, once for the benefit with regard to death, once for the benefit related

to SARS-CoV-2 infection and possibly for the benefit concerning COVID-19 related hospitalisation and/or ICU admission.

3. Efficacy and safety are usually analysed separately, possibly using different data sources, and the results of these analyses are combined in a quantitative benefit-risk assessment, ignoring the possible association between efficacy and safety events.

Within the domain of decision theory, the closely related disadvantages #2 and #3 can, possibly, be taken into account via extensions of SMAA models for correlated criteria [54, 55] or via more complex, non-additive MCDA models. The SMAA extensions, however, have not seen many practical applications, while the latter requires additional preference parameters and thus a more complex preference elicitation process, making its practical feasibility questionable.

In the clinical trials setting, it has been long recognized and criticised that benefit-risk composite measures ignore the association between benefit and risks [56, 57]. Although several remedial measures have been proposed, they all have the disadvantage of requiring data at an individual subject level, making these methods often unpractical outside the clinical trial setting, where frequently only data at an aggregated level is available.

However, one particular method, the prioritized Generalized Pairwise Comparison (GPC) may potentially offer an alternative to remediate all disadvantages of the INHB and support decision making next to quantitative MCDA.

GPC has originally been proposed as a flexible statistical method to analyse multiple outcomes simultaneously for the comparison of a treatment group and a control group [58, 59, 60]. Prioritized GPC requires outcomes to be ranked, usually the most severe is ranked first, which circumvents the difficulty of defining weights for the outcomes of interest and allows for the combination of any type and number of outcomes. The GPC statistics are based on comparing outcomes for all pairs of patients, formed by taking one patient from the treatment group and one patient from the control group and assigning a winner or tie in each pair based on the prioritized outcomes. When a winner can be assigned per pair, outcomes further down in the priority list are not evaluated, hence preventing multiple counting if the benefits of COVID-19 vaccination would be ranked: death, ICU admission, hospitalisation and infection. Both absolute (net benefit [58]) and relative (win odds [61], win ratio [59]) measures have been proposed, with a relatively straightforward interpretation. Prioritized benefit-risk assessment with GPC has recently been suggested in oncology trials, showing its benefit of taking account of the correlation between events compared to the summing of marginal effects such as in INHB [62, 63, 64]. Although GPC requires individual subject data, a straightforward calculation of the prioritized net benefit is available when independent proportions of an event are considered [65]. Thus, when using independent incidence proportions or cumulative incidences rather than incidence rates, a direct calculation of the prioritized GPC is possible:

$$\text{net benefit} = \sum_{i=1}^{n} (P_{0i} - P_{vi}) \prod_{h=1}^{n-i} \left[P_{0h} P_{vh} + (1 - P_{0h})(1 - P_{vh}) \right],$$

with $n = k + l$, the total number of risks and benefits, and P_0 and P_v representing the proportion of each benefit and risk in the unvaccinated and vaccinated population, respectively.

The additional advantage of GPC (over other measures) is that the net benefit value lays between -1 and 1, which makes values comparable and more easily interpretable, thereby solving issue 1. discussed above.

Additionally, relative measures such as the win ratio and win odds are available. Note that when incidence proportions rather than incidence rates are used as utility measure in the INHB, a statistic is obtained that is comparable to non-prioritized GPC [60].

In summary, current benefit-risk assessment methods ignore correlation between benefit and risk events, count overlapping events multiple times in linear value functions and result in a benefit-risk value that depends on the number of benefit and risk events. The first two issues may be solved by expanding the well-known MCDA and SMAA models to accommodate correlated events. However these extended models have not been applied often in benefit-risk assessment and may suffer from additional complexities of assigning weights. All issues of current benefit-risk assessment methods may be solved by applying prioritized GPC, which has the additional benefit that no weights elicitation is required. However, prioritized GPC has only been very recently presented as a benefit-risk assessment tool and it requires independent incidence proportions for all events.

Further research is required to investigate the performance of each of the proposed methods in the context of correlated and possible duplicate events in detail. Ultimately, prioritized GPC is another potential decision tool, that should be used alongside more traditional benefit-risk analyses to aid evaluation of benefit and risk.

9 Limitations

In this report, the benefit-side of vaccination is based on the probabilistic model (see PM above), albeit the application of the stochastic compartmental model (referred to as SCM above) is a more refined though complex model to quantify these benefits. Due to data sparseness and computational complexity it remains challenging to inform the SCM and to achieve converge for all model parameters and all countries. Nonetheless, while the SCM is currently still under construction, it will be considered in future updates of the aforementioned analyses.

The PM suffers from some **limitations**. Although it is based on a direct quantification of the prevented cases, hospitalizations, ICU admissions and deaths, the current application of the PM does not provide an assessment of uncertainty. However, this feature is implicitly available through the repeated use of the Shiny R app enabling a user-defined Monte Carlo simulation including a range of user-specified parameter values. Next to that, the PM does not account for build-up of natural immunity in the absence of vaccine-induced immunity. The inclusion of this feature would imply a recursive assessment of the impact of vaccination over time, given that the prevention of (confirmed) COVID-19 cases at calendar time t in age group a, will have an impact on natural immunity levels at subsequent time points. Although such a recursive assessment would be possible and the inclusion of natural immunity is methodologically straightforward, such country-specific computations are computer-intensive thereby potentially jeopardising the usefulness of the Shiny R app. Moreover, as individual-level data on the time between consecutive vaccination doses is missing, we approximate the protection induced by vaccination against infection, hospitalization, ICU admission and death at the population level. More specifically, a gradual build-up of vaccine protection after first, second and booster vaccination is accounted for, though the aggregation of protection over time is performed without explicitly accounting for time between consecutive doses. This implies that we assume that the time between such doses is random. Finally, in the absence of time- and age-dependent information

concerning hospitalizations, ICU admissions and deaths at the country-level, the quantification of prevented hospitalizations, ICU admissions and deaths in the PM is based on a time-invariant age distribution estimated for each of these endpoints separately over the entire course of the epidemic. However, the prevented burden is therefore potentially overestimated as the temporal protective and beneficial effects of vaccination in age groups with high vaccine uptake are averaged out. This further underlines the importance of the availability of detailed age- and time-specific information to improve estimation of the prevented burden.

A **limitation in the risk assessment** is the, potentially arbitrary, manually chosen weight to assign more value to one source of background incidence rates compared to another source. To exclude the arbitrariness, an alternative could be to use a variation on the weighted least square method, where the inverse variance weight is multiplied with a factor that is based on Cochran's Q heterogeneity measure [66]. However, the incidence rate will be the same as under equal weighting, while the variance or imprecision will increase [66]. Alternatively, a formal sensitivity analysis can be performed by providing several weighting scenarios to the Shiny R application, as demonstrated in this report.

A **limitation in the myocarditis risk assessment** is the exclusion of vaccine coverage data with unknown age or vaccine in the ECDC vaccine coverage data set. The exclusion on a country level is quite substantial for Poland (∼92,000 vaccines excluded) and Croatia (∼16,000) slightly less for Austria (∼4,000), France (∼3,200) (Bulgaria (∼2,000) and The Netherlands (∼1,300), and negligible for Denmark, Estonia, Greece, Ireland, Iceland, Lithuania, Latvia, Portugal and Slovakia (between 2 and 462). The actual vaccine coverage is thus actually higher than the coverage used in the risk assessment and the Observed-Expected ratios potentially smaller than reported. The impact on the conclusions is, however, deemed minor, given it concerns only 0.07% of all administered vaccines (∼120,000 on ∼178,000,000). To include the administered doses with unknown age or vaccine, a redistribution as applied before can be applied.

In general, the result of the study can be achieved by combining different data sources (i.e., EMA, ECDC, TESSy, EudraVigilance, etc.) in which many difficulties (i.e., weighting, missing data, heterogeneous data structure, etc.) were encountered. These can be avoided by having better data quality, which reduces the complexity of the analysis and improves the quality of the results. A more straightforward method will be possible with a national dataset. This is a challenge for the EU and its Member States, as different granularity in data collection and surveillance systems still exists.

10 Conclusion

The benefit of the mRNA and adeno-based COVID-19 vaccines are demonstrated by the estimated prevention of a total of 13,322,567 confirmed COVID-19 infections, 933,230 COVID-19 hospitalizations, 150,106 ICU admissions and 220,880 COVID-19 related deaths since the start of the COVID-19 vaccination program in the different European countries. The prevention of the COVID-19 related clinical events outweighs the associated myocarditis and TTS risks with mRNA and adeno-based vaccine respectively in each age category. The observed-expected myocarditis risk analysis shows a decreased myocarditis risk after vaccination when compared to the COVID-19 pandemic period prior to the introduction of vaccination, except for

males between 18–29 years vaccinated with Spikevax in which an increased risk is observed. In general the risk of myocarditis is higher after Spikevax vaccination compared to Cominarty vaccination. In the age categories < 40y the risk of myocarditis after vaccination is slightly higher in males compared to females.

References

[1] World Health Organization. *WHO Coronavirus (COVID-19) Dashboard*, 2021. https://covid19.who.int/.

[2] C. Whittaker, P.G. Walker, M. Alhaffar, A. Hamlet, B.A. Djaafara, A. Ghani, N. Ferguson, M. Dahab, F. Checchi, and O.J. Watson. Under-reporting of deaths limits our understanding of true burden of covid-19. *BMJ*, 375, 2021.

[3] N. Hens, P. Vranckx, and G. Molenberghs. The COVID-19 epidemic, its mortality, and the role of non-pharmaceutical interventions. *European Heart Journal: Acute Cardiovascular Care*, 9(3):204–208, 2020.

[4] G. Molenberghs, M. Buyse, S. Abrams, N. Hens, P. Beutels, C. Faes, and others. Infectious diseases epidemiology, quantitative methodology, and clinical research in the midst of the COVID-19 pandemic: Perspective from a European country. *Contemporary clinical trials*, 99:106189, 2020.

[5] European Centre for Disease Prevention and Control. *Risk of SARS-CoV2 transmission from newly infected individuals with documented previous infection or vaccination.*, 2021. https://www.ecdc.europa.eu/en/publications-data/sars-cov-2-transmission-newly-infected-individuals-previous-infection.

[6] European Centre for Disease Prevention and Control. *Weekly COVID-19 country overview.*, 2021. https://covid19-country-overviews.ecdc.europa.eu/.

[7] European Medicines Agency. *AstraZeneca's COVID-19 vaccine: EMA finds possible link to very rare cases of unusual blood clots with low blood platelets*, 2021. https://www.ema.europa.eu/en/news/astrazenecas-covid-19-vaccine-ema-finds-possible-link-very-rare-cases-unusual-blood-clots-low-blood.

[8] European Medicines Agency. *COVID-19 Vaccine Janssen: EMA finds possible link to very rare cases of unusual blood clots with low blood platelets.*, 2021. https://www.ema.europa.eu/en/news/covid-19-vaccine-janssen-ema-finds-possible-link-very-rare-cases-unusual-blood-clots-low-blood.

[9] European Medicines Agency. *COVID-19 vaccines: update on ongoing evaluation of myocarditis and pericarditis.*, 2021. https://www.ema.europa.eu/en/news/covid-19-vaccines-update-ongoing-evaluation-myocarditis-pericarditis.

[10] S. M. Moghadas, T. N. Vilches, K. Zhang, S. Nourbakhsh, P. Sah, M. C. Fitzpatrick, and A. P. Galvani. Evaluation of covid-19 vaccination strategies with a delayed second dose. *PLoS biology*, 19(4):e3001211, 2021.

[11] J. M. Caldwell, X. Le, L. McIntosh, M. T. Meehan, S. Ogunlade, R. Ragonnet, G. K. O'Neill, J. M. Trauer, and E. S. McBryde. Vaccines and variants: Modelling insights into emerging issues in covid-19 epidemiology. *Paediatric Respiratory Reviews*, 39:32–39, 2021.

[12] S. Khare, C. Gurry, L. Freitas, M.B. Schultz, G. Bach, A. Diallo, N. Akite, J. Ho, R.T.C. Lee, W. Yeo, et al. Gisaid's role in pandemic response. *China CDC Weekly*, 3(49):1049, 2021.

[13] S. Elbe and G. Buckland-Merrett. Data, disease and diplomacy: Gisaid's innovative contribution to global health. *Global challenges*, 1(1):33–46, 2017.

[14] Y Shu and J McCauley. Eurosurveillance 2017, doi: 10.2807/1560-7917, 2017.

[15] S.N. Wood. *Generalized additive models: an introduction with R*. chapman and hall/CRC, 2006.

[16] P. Krause, T.R. Fleming, I. Longini, A. M. Henao-Restrepo, R. Peto, N.E. Dean, M.E. Halloran, Y. Huang, T.R. Fleming, P.B. Gilbert, et al. Covid-19 vaccine trials should seek worthwhile efficacy. *The Lancet*, 396(10253):741–743, 2020.

[17] C.B. Creech, S.C. Walker, and R.J. Samuels. Sars-cov-2 vaccines. *Jama*, 325(13):1318–1320, 2021.

[18] J.L. Bernal, N. Andrews, C. Gower, E. Gallagher, R. Simmons, S. Thelwall, J. Stowe, E. Tessier, N. Groves, G. Dabrera, et al. Effectiveness of covid-19 vaccines against the b. 1.617. 2 (delta) variant. *New England Journal of Medicine*, 2021.

[19] J. Stowe, N. Andrews, ..., and J. L. Bernal. Effectiveness of COVID-19 vaccines against hospital admission with the delta (B.1.617.2) variant. *preprint*, pages 1–3, 2021.

[20] N. Andrews, J. Stowe, F. Kirsebom, S. Toffa, R. Sachdeva, C. Gower, M. Ramsay, and J. L. Bernal. Effectiveness of covid-19 booster vaccines against covid-19 related symptoms, hospitalisation and death in england. *Nature medicine*, pages 1–1, 2022.

[21] K. J Bruxvoort, L. S. Sy, L. Qian, B. K Ackerson, Y. Luo, G. S. Lee, Y. Tian, A. Florea, M. Aragones, J. E. Tubert, et al. Effectiveness of mrna-1273 against delta, mu, and other emerging variants of sars-cov-2: test negative case-control study. *bmj*, 375, 2021.

[22] Nick Andrews, Elise Tessier, Julia Stowe, Charlotte Gower, Freja Kirsebom, Ruth Simmons, Eileen Gallagher, Meera Chand, Kevin Brown, Shamez N Ladhani, Mary Ramsay, and Jamie Lopez Bernal. Vaccine effectiveness and duration of protection of comirnaty, vaxzevria and spikevax against mild and severe covid-19 in the uk. *medRxiv*, 2021.

[23] R. Sonabend, L. K. Whittles, N. Imai, P. N. Perez-Guzman, E. S. Knock, T. Rawson, K.A.M. Gaythorpe, B. A. Djaafara, W. Hinsley, R.G. FitzJohn, et al. Non-pharmaceutical interventions, vaccination, and the sars-cov-2 delta variant in england: a mathematical modelling study. *The Lancet*, 398(10313):1825–1835, 2021.

[24] Innovative Medicines Initiative. *Accelerated development of vaccine benefit-risk collaboration in Europe*, 2021. https://www.imi.europa.eu/projects-results/project-factsheets/advance.

[25] Centres for Disease Control and Prevention. *Population-Level Risk-Benefit Analysis*, 2021. https://www.cdc.gov/vaccines/covid-19/info-by-product/janssen/risk-benefit-analysis.html.

[26] S. Abrams, J. Wambua, E. Santermans, L. Willem, E. Kuylen, P. Coletti, and others. Modeling the early phase of the Belgian COVID-19 epidemic using a stochastic compartmental model and studying its implied future trajectories. *Epidemics*, 35:100449, 2021.

[27] J. Wallinga, P. Teunis, and M. Kretzschmar. Using data on social contacts to estimate age-specific transmission parameters for respiratory-spread infectious agents. *American journal of epidemiology*, 164(10):936–944, 2006.

[28] N. Hens, Z. Shkedy, M. Aerts, C. Faes, P. Van Damme, and P. Beutels. *Modeling infectious disease parameters based on serological and social contact data: a modern statistical perspective*, volume 63. Springer Science & Business Media, 2012.

[29] J.J. Deeks, J.P.T. Higgins, and Altman D.G. Cochrane handbook for systematic reviews of interventions version 6.2 (updated february 2021), 2021. Available from https://www.training.cochrane.org/handbook.

[30] E.B. Wilson and M.M. Hilferty. The distribution of Chi-square. *Proc Natl Acad Sci USA*, 17:684–8, 1931.

[31] K.J. Rothman and J.D. Boice. *Epidemiologic Analysis with a Programmable Calculator*. Boston, MA: Epidemiology Resources, Inc, 1982.

[32] E. Vasileiou, C. R. Simpson, C. Robertson, T. Shi, S. Kerr, U. Agrawal, A. Akbari, S. Bedston, J. Beggs, D. Bradley, et al. Effectiveness of first dose of covid-19 vaccines against hospital admissions in scotland: national prospective cohort study of 5.4 million people. 2021.

[33] International Society on Thrombosis and Haemostasis. *ISTH GLOBAL RESPONSE TO COVID-19*, 2021. https://www.isth.org/page/covid19.

[34] J. Juhaeri. Benefit–risk evaluation: the past, present and future. *Ther Adv Drug Saf*, pages 1–10, 2019.

[35] H. Arlegui, K. Bollaerts, F. Salvo, V. Bauchau, G. Nachbaur, B. Bégaud, and N. Praet. Benefit–risk assessment of vaccines. part i: A systematic review to identify and describe studies about quantitative benefit–risk models applied to vaccines. *Drug Safety*, page 1089–1104, 2020.

[36] European Medicines Agency (EMA). *Benefit-risk methodology project work package 2 report: Applicability of current tools and processes for regulatory benefit-risk assessment. London: European Medicines Agency.*, 2010. http://www.ema.europa.eu/docs/en_GB/document_library/Report/2010/10/WC500097750.pdf.

[37] European Medicines Agency (EMA). *Benefit-risk methodology project work package 3 report: Field tests. London: European Medicines Agency.*, 2011. http://www.ema.europa.eu/docs/en_GB/document_library/Report/2011/09/WC500112088.pdf.

[38] *Pharmacoepidemiological Research on Outcomes of Therapeutics by a European Consortium (PROTECT) Benefit Risk website*. http://protectbenefitrisk.eu/index.html.

[39] N. McAuslane, J. Leong, L. Liberti, and S. Walker. The benefitrisk assessment of medicines: experience of a consortium of medium-sized regulatory authorities. *Ther Innov Regul Sci.*, 51(5):635–4, 2017.

[40] J.J. Guo, S. Pandey, J. Doyle, B. Bian, Y. Lis, and D.W. Raisch. A review of quantitative risk-benefit methodologies for assessing drug safety and efficacy-report of the ISPOR risk-benefit management working group. *Value Health*, 13(5):657–66, 2010.

[41] P. Thokala, N. Devlin, K. Marsh, R. Baltussen, M. Boysen, Z. Kalo, T. Longrenn, F. Mussen, S. Peacock, J. Watkins, and M. Ijzerman. Multiple criteria decision analysis for health care decision making—an introduction:report 1 of the ispor mcda emerging good practices task force. *Value in Health*, page 1–13, 2016.

[42] K. Marsh, M. Ijzerman, P. Thokala, R. Baltussen, M. Boysen, Z. Kalo, T. Longrenn, F. Mussen, S. Peacock, J. Watkins, and N. Devlin. Multiple criteria decision analysis for health care decision making—emerging good practices:report 2 of the ispor mcda emerging good practices task force. *Value in Health*, page 125–137, 2016.

[43] K. Bollaerts, B. V. Vincent, E. Ledent, B. Levitan, T. Verstraeten, and Y. Zhong. *Accelerated Development of VAccine beNefit-risk Collaboration in Europe. Work package 4, D4.3 Report on appraisal of vaccine benefit-risk methodology*, 2014. https://vac4eu.org/wp-content/uploads/2019/03/ADVANCE_D4.3appraisal_benefit_risk-methods.pdf.

[44] H. Arlegui, K. Bollaerts, V. Bauchau, G. Nachbaur, B. Bégaud, and N. Praet. Benefit-risk assessment of vaccines. part ii: Proposal towards consolidated standards of reporting quantitative benefit-risk models applied to vaccines (brivac). *Drug Safety*, page 1105–1120, 2020.

[45] F. Mussen, S. Salek, and S. Walker. *Benefit-risk appraisal of medicines: a systematic approach to decision-making*. Chichester: John Wiley & Sons, 2009.

[46] K. Bollaerts, E. Ledent, T. de Smedt, D. Weibel, HD. Emborg, G. Danieli, et al. ADVANCE system testing: Benefit-risk analysis of a marketed vaccine using multi-criteria decision analysis and individual-level state transition modelling. *Vaccine*, 38:B65–B75, 2020.

[47] K. Bollaerts, T. de Smedt, K. Donegan, L. Titievsky, and V. Bauchau. Benefit–risk monitoring of vaccines using an interactive dashboard: A methodological proposal from the ADVANCE project. *Drug Saf*, 41:775–786, 2018.

[48] T.L. Saaty. A scaling method for priorities in hierarchical structures. *Journal of Mathematical Psychology*, 15(3):234–281, 1977.

[49] C. A. B. e Costa and J.C. Vansnick. MACBETH: An interactive path towards the construction of cardinal value functions. *International Transactions in Operational Research*, 1(4):489–500, 1994.

[50] R. Lahdelma and P. Salminen. Smaa-2: Stochastic multicriteria acceptability analysis for group decision making. *Operations Research*, 49(3):444–454, 2001.

[51] T. Tervonen, G. van Valkenhoef, E. Buskens, H.L. Hillege, and D. Postmus. A stochastic multicriteria model for evidence-based decision making in drug benefit-risk analysis. *Statistics in Medicine*, 30:1419–1428, 2011.

[52] M.F. Drummond, M.J. Sculpher, K. Claxton, G.L. Stoddart, and GW. Torrance. *Methods for the economic evaluation of health care programmes*. Oxford University Press, 2005.

[53] L.D. Lynd, M. Najafzadeh, L. Colley, M.F. Byrne, A.R. Willan, M.J. Sculpher, et al. Using the incremental net benefit framework for quantitative benefit-risk analysis in regulatory decision-making–a case study of alosetron in irritable bowel syndrome. *Value Health*, 13(4):411–7, 2010.

[54] R. Lahdelma, S. Makkonen, and P. Salminen. Multivariate gaussian criteria in SMAA. *European Journal of Operational Research*, 170:957–970, 2006.

[55] R. Lahdelma, S. Makkonen, and P. Salminen. Two ways to handle dependent uncertainties in multi-criteria decision problems. *Omega*, 37(1):79–92, 2009.

[56] S.R. Evans and D. Follmann. Using outcomes to analyze patients rather than patients to analyze outcomes: a step toward pragmatism in benefit: risk evaluation. *Stat Biopharm*, 8:386–393, 2016.

[57] P.A. Shaw. Use of composite outcomes to assess risk–benefit in clinical trials. *Clinical Trials*, 15:352–358, 2018.

[58] M. Buyse. Generalized pairwise comparisons of prioritized outcomes in the two-sample problem. *Stat Med*, 29:3245–3257, 2010.

[59] S. Pocock, C. Ariti, T. Collier, and others. The win ratio: a new approach to the analysis of composite endpoints in clinical trials based on clinical priorities. *Eur Heart J*, 33:176–182, 2012.

[60] J. Verbeeck, E. Spitzer, T. de Vries, G. van Es, W. Anderson, N. Van Mieghem, et al. Generalized pairwise comparison methods to analyze (non)prioritized composite endpoints. *Stat Med*, 38:5641–5656, 2019.

[61] E. Brunner, M. Vandemeulebroecke, and T. Mütze. Win odds: An adaptation of the win ratio to include ties. *Stat Med*, 40:3367– 3384, 2021.

[62] J. Peron, P. Roy, K. Ding, and others. Assessing the benefit-risk of new treatments using generalised pairwise comparisons: the case of erlotinib in pancreatic cancer. *Br J Cancer*, 112:971–976, 2015.

[63] J. Peron, P. Roy, T. Conroy, and others. An assessment of the benefit-risk balance of folfirinox in metastatic pancreatic adenocarcinoma. *Oncotarget*, 7:82953–82960, 2016.

[64] M Buyse, E.D. Saad, J. Peron, J.C. Chiem, M. De Backer, E. Cantagallo, and O. Ciani. The net benefit of a treatment should take the correlation between benefits and harms into account. *Journal of Clinical Epidemiology*, 137:148–158, 2021.

[65] G. Rauch, A. Jahn-Eimermacher, W. Brannath, and M. Kieser. Opportunities and challenges of combined effect measures based on prioritized outcomes. *Stat Med*, 33:1104–1120, 2014.

[66] M. Pathaka, S.N. Dwivedib, B. Thakura, and S. Vishnubhatla. Methods of estimating the pooled effect size under meta-analysis: A comparative appraisal. *Clinical Epidemiology and Global Health*, 8:105–112, 2020.